THESIS

$2\mathcal{85}68428$
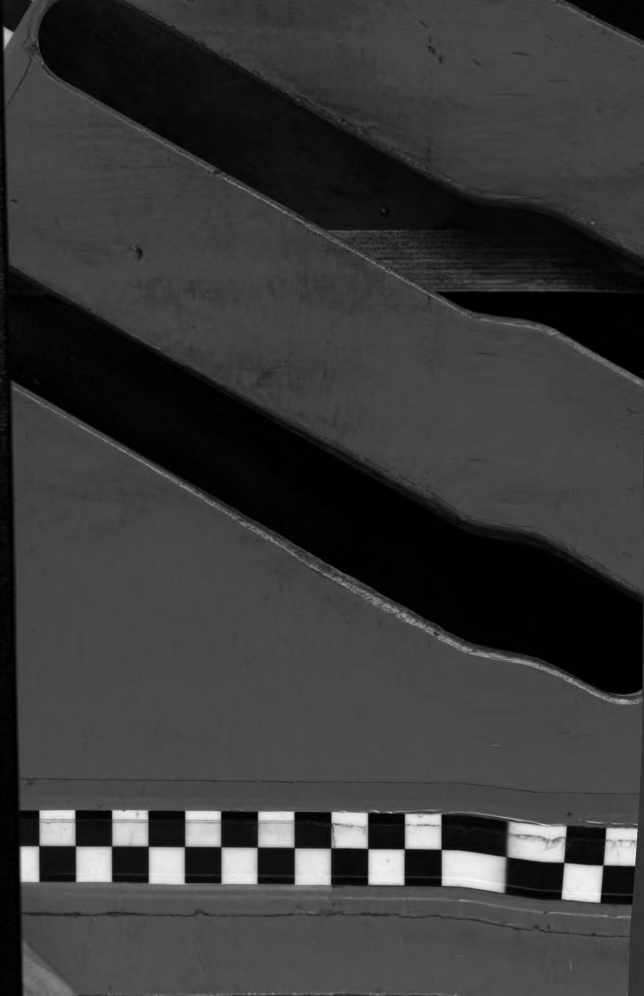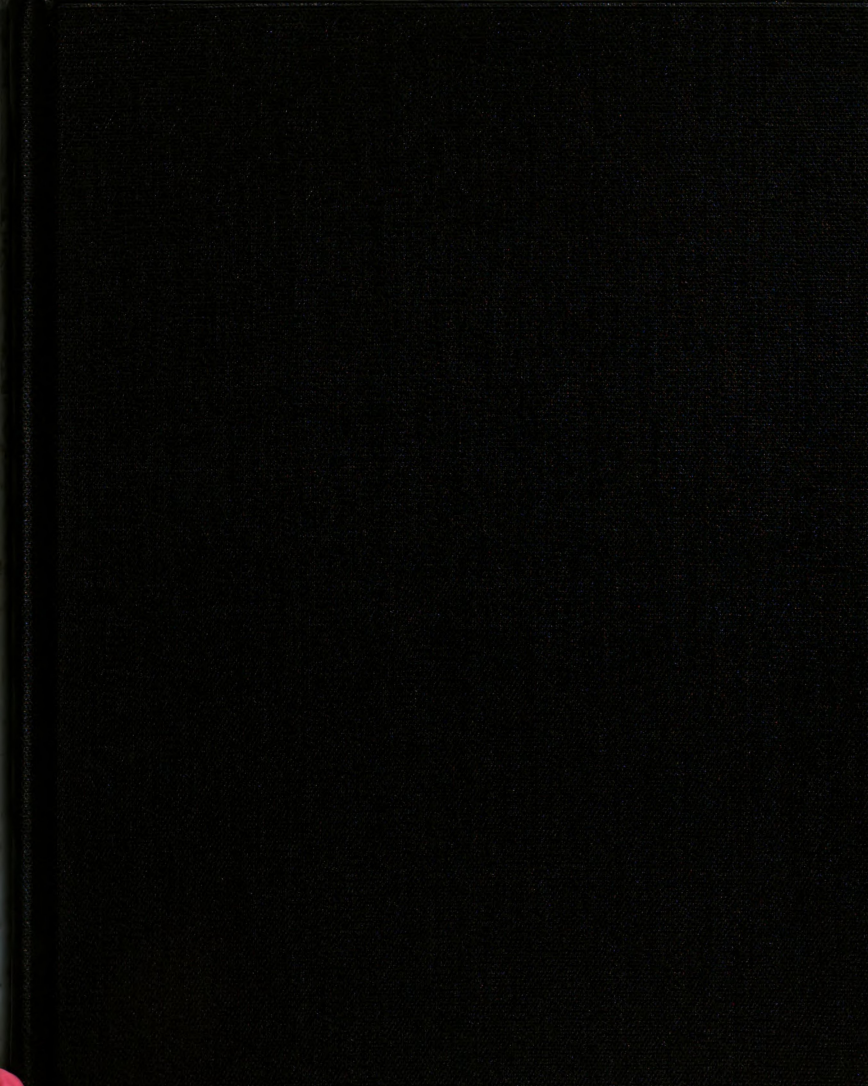
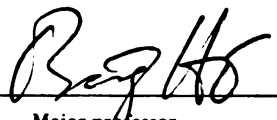This is to certify that the

thesis entitled

NON-INVASIVE TEMPERATURE MEASUREMENT
BY ULTRASCNIC TECHNIQUES

presented by

Di Ye

has been accepted towards fulfillment
of the requirements for

____M. S.____ degree in __Electrical__ Engineering

Major professor

Date __June 26, 1989__

PLACE IN RETURN BOX to remove this checkout from your record.
TO AVOID FINES return on or before date due.

DATE DUE	DATE DUE	DATE DUE
_____	_____	_____
_____	_____	_____
_____	_____	_____
_____	_____	_____
_____	_____	_____
_____	_____	_____
_____	_____	_____

MSU Is An Affirmative Action/Equal Opportunity Institution

c:\circ\datedue.pm3-p.1

NON-INVASIVE TEMPERATURE MEASUREMENT

BY ULTRASONIC TECHNIQUES

By

Di Ye

A THESIS

Submitted to

Michigan State University

in partial fulfillment of the requirements

for the degree of

MASTER OF SCIENCE

Department of Electrical Engineering and Systems Science

1989

ABSTRACT

NON-INVASIVE TEMPERATURE MEASUREMENT

BY ULTRASONIC TECHNIQUES

By

Di Ye

Non-invasive temperature measurement utilizing a micro-computer based ultrasonic imaging system for in- vitro tissue studies has been investigated. This work is based on the theory that the velocity of ultrasound in a medium is a function of temperature, and on previous experimental results of temperature dependent sensing in biological tissues. The work reported here represents a special technique developed recently to monitor the relative temperature change in tissues in a simulated hyperthermia treatment situation. The technique involves wave pattern matching to detect the echo phase change due to temperature variation in the tissue. A 40 MHz sampling rate data aquisition system is used to obtain high resolution in velocity change so that a $0.2^o C$ temperature change may be identified. Temperature profile imaging of an experimental model has been obtained. The techniques used and experimental results obtained are presented.

Acknowledgements

I wish to thank Dr. Bong Ho, my advisor, for his timely guidance and support. I wish to thank Dr. H. Roland Zapp and Dr. R. O. Barr for their suggestions relevant to this research.

I wish to thank Mr. Nai Hsien Wang and Mr. Mo Zhang for their aid in the use of the computer software developed in the Ultrasound Research Laboratory and in assistance with equipment operation. I would like to thank my parents and my wife for their constant help and encouragement.

Table of Contents

List of Tables

List of Figures

CHAPTER 1

Introduction

Non-invasive temperature monitoring has many important applications in areas of hyperthermia treatment of cancer, studying physical properties of materials, power generation and nuclear reactor safety monitoring.

The use of focused ultrasound to induce localized hyperthermia in malignant tissue is currently being investigated in many places. The purpose of these investigations is to selectively damage malignant tissue in order to inhibit its growth and ultimately cause its disappearance. The ideal temperature for hyperthermia treatment is to have the tumor at the threshold level (42.5^0C) or above and the surrounding healthy tissues at normal levels (37^0C). Temperature distributions have been produced in tissue which come very near to this desired distribution so that lab experiment may be performed [1].

During hyperthermia the treated region requires accurate temperature monitoring to ensure that normal tissue is not damaged. Current practice is to insert thermocouples or thermistors encased in hypodermic needles to make the necessary measurements. The invasiveness of this technique limits the number of temperature probes used and in some cases makes it very

cumbersome because repeated insertion can result in other hazards such as infection and tissue destruction. In addition, placing temperature probes into the treated region often complicates the heating process [2]. A method of monitoring the temperature rise during hyperthermia without intrusion into the body would clearly be beneficial.

Non-invasive temperature measurements are also widely used to determine properties and states of materials. There has been an increasing use of ultrasonic temperature measurements for nondestructive characterization of material microstructures and mechanical properties. Therefore, it is important to have appropriate practical methods for making temperature measurements for a variety of purposes.

A number of approaches to non-invasive temperature measurement have been used. Among the approaches are those that use single-frequency continuous waves, tone bursts, and broadband pulse-echo waveforms. In the latter case, the basic problem is to determine the time delay between successive echoes, from which the velocity change as a function of temperature could be measured. The pulse-echo approach using a single transducer as both transmitter and receiver has many practical advantage over the transmission methods and therefore will be treated exclusively in this thesis.

The measurement technique developed in this thesis is theoretically

based on the ultrasonic velocity as a function of temperature. The technique is also based on computer digitization of broadband pulse-echo waveforms. A number of software routines have been implemented in the ultrasonic imaging system in the Ultrasonic Research Laboratory for the purpose of non-invasive temperature measurement.

The immediate objectives of the work reported here are to monitor temperature distributions inside a layered material and to obtain temperature profiles of experimental models with well-defined boundary and temperature gradients. The work described here provides a base for future research and applications in medicine and engineering. This research is to seek the feasibility of using ultrasound as a supplemental or primary mode of non-invasive temperature monitoring during simulated hyperthermia treatment. Techniques to be developed include the use of higher data sampling rate, calibration of standard materials for absolute temperature mapping.

The most common used medical imaging techniques use X-rays or ultrasound. X-ray technology, including CAT scans, and ultrasound technology present images which essentially show differences in density. This is generally easy to visualize. (More specifically, ultrasonic B-scan images show sharp differences in the acoustic impedance ρc, or density times propagation velocity and radiography using X-ray radiation shows the spatial distribution of X-ray attenuation coefficients which are highly density

dependent.) The difficulty with any thermal imaging technique is to present an image with various temperature gradients. For infra-red imaging, digital signal processing techniques are used for color coding to display the regions of different temperature. This type of imaging display could very well be employed by ultrasonic non-invasive temperature monitoring.

The contents of this thesis are organized as follows. First, the theoretical foundations of the temperature dependence of ultrasound propagation are reviewed. Second, judging from published research results, theoretical considerations for temperature monitoring will be described as the experimental basis. Third, a variety of non-invasive temperature measurement techniques are briefly described for overviewing and comparison. The remainder of the thesis will devote to the details of the research work in ultrasonic temperature monitoring, including system configuration, experiment design, result and analysis. The system limitations and suggestions for future study will also be discussed.

CHAPTER 2

Theoretical Consideration

This chapter provides the necessary theoretical background for the proposed techniques of non-invasive measurement of temperature . In the first section, some related ultrasound principles are reviewed. It is followed by the theoretical foundations of ultrasonic propagation on temperature profiles. Some new measurement techniques are proposed and implemented based on literature review and laboratory experiments.

2.1 Review of Ultrasound Principles

It is useful to examine the theoretical foundations of temperature dependence on ultrasonic propagation. This information is well documented in the literature and is included here for completeness and convenience.

2.1.1 Wave Motion

Ultrasonic energy travels through a medium in the form of shear and longitudinal waves. The simplest type to be studied is a longitudinal single frequency displacement in an isotropic medium which is perfectly elastic. The energy is transmitted continuously, and the vibration is simple

harmonic lattice displacement about a mean particle position. A particle is an element of volume which is continuous with its surroundings, but small enough for quantities which are variable within the medium to be constant within the particle. The movement of the particles is resisted by elastic forces due to the molecular structure of the medium.

Let us consider plane, non-spreading longitudinal waves. The displacement amplitude u from the mean position of particles in simple harmonic motion, at any instant t, and at a fixed point along the direction of the wave, where $u=0$ when $t=0$, is given by

$$u = u_0 \sin\omega t \qquad (2.1.1)$$

where u_0= maximum displacement amplitude, and $\omega=2\pi f$, where f is the frequency of the wave.

Velocity is equal to rate of change of position, and so it may be found by differentiating the particle displacement with respect to time. Thus

$$v = \frac{\partial u}{\partial t} = u_0 \omega \cos\omega t \qquad (2.1.2)$$

Similarly, the acceleration a of the particle towards its mean position may be found by differentiating the particle velocity with respect to time. Thus

$$a = \frac{\partial v}{\partial t} = -u_0 \omega^2 \sin\omega t \qquad (2.1.3)$$

The significance of the negative sign is that the particle is decelerating as it moves away from its mean position.

From Equations (2.1.1),(2.1.2) and (2.1.3), the phase of the particle velocity leads that of the particle displacement by a time interval corresponding to $\frac{\pi}{2}$ radians of phase-angle difference, while the acceleration is π out of phase with the displacement.

Ultrasonic energy is transported by mechanical vibrations at frequencies above the upper limit of human audibility. The ultrasound consists of a propagating periodic disturbance in the elastic medium, causing the particles of the medium to vibrate about their mean (equilibrium) positions. The vibratory motion of the particles is essential to energy propagation. The transmission through the medium is strongly dependent on the ultrasound frequency, temperature and the state of the medium such as gas, liquid, or solid. The velocity values listed in Table (2.1.1) are under the assumption of constant temperature of some fixed value. The table illustrates the velocity dependency on the medium composition.

Below some temperature, the speed at which ultrasonic vibrations are transmitted through a medium is inversely proportional to the square root of the product of the density and the adiabatic compressibility of the material. The speed of sound (c), along with frequency (f) determine

Table 2.1.1 Approximate values of ultrasonic velocities of various media [1]

Medium	Sound Velocity (m/sec)
Dry air $(20^0C)\%343.6$	
Water $(37^0C)\%1524$	
Amniotic fluid	1530
Brain	1525
Fat	1485
Liver	1570
Muscle	1590
Tendon	1750
Skull bone	3360
Uterus	1625

the wavelength (λ), from the relationship

$$\lambda = \frac{c}{f} \qquad (2.1.4)$$

The knowledge of the speed at which ultrasound is transmitted through a medium is used in the conversion of echo-return time into depth of material being imaged.

2.2 The temperature dependence of ultrasonic propagation

It is important to realize that, although energy is transmitted through the medium as the result of a wave motion, no net movement of the medium is required for this to occur.

In reality, the whole of the curve in Figure (2.1.1) is moving forward with a velocity c, which is measured by the distance which any particular part of the curve travels in unit time. For this reason, it is sometimes called a travelling or progressive wave. The phase of the wave indicates in what part of the vibrational cycle the wave happens to be at any particular instant of time. The transmission of the disturbance is not infinitely fast, because a delay occurs between the movements of neighbour particles. The velocity of propagation is controlled by the density of the medium and its elasticity. The relationship depends upon the kind of material and the wave mode. It can be shown that, for longitudinal waves in fluids

$$c = \sqrt{\frac{K_a}{\rho}} \qquad (2.2.1)$$

where K_a = adiabatic bulk modulus, and ρ = mean density of medium.

The adiabatic bulk modulus (which is the reciprocal of the adiabatic compressibility) is not the same as the isothermal bulk modulus K_i

obtained by static measurements, although for most liquids the two quantities are almost equal. Thus

$$K_a = \gamma K_i \qquad (2.2.2)$$

where γ = the ratio of specific heat at constant pressure to that at constant volume.

In the case of longitudinal bulk waves in isotropic solids, the situation is complicated by the fact that the shear rigidity of the medium couples some of the energy of the longitudinal wave into a transverse mode. The appropriate modulus for calculating the velocity contains not only a term which depends upon the bulk modulus, but also one which depends upon the shear modulus. The formula is

$$c = \sqrt{\frac{K+1.33G}{\rho}} \qquad (2.2.3)$$

where G = shear modulus.

The bulk and shear moduli are related to Young's modulus Y and Poisson's ratio σ as follows:

$$K = \sqrt{\frac{Y}{3(1-2\sigma)}}$$

$$G = \sqrt{\frac{Y}{2(1+\sigma)}}$$

Substitution of these values in Equation (2.7) gives

$$c = \sqrt{\frac{Y(1-\sigma)}{(1-2\sigma)(1+\sigma)\rho}} \qquad (2.2.4)$$

The elastic constants are temperature-dependent, and so the velocity alters with temperature. The relationship can be quite complicated; for example, Figure (2.2.1) shows the temperature variation of the velocity of ultrasound in distilled water at atmospheric pressure.

The temperature dependency of ultrasound has been also investigated by Isaak Elpiner [3], who provided the basic laws governing the propagation of ultrasound waves in gases, liquids, and solids.

The velocity of sound waves c in gases is given by the Laplace formula if the amplitude of the vibrations is relatively small:

$$c = \sqrt{\frac{\gamma P}{\rho}} = \sqrt{\frac{\gamma}{M}RT} \qquad (2.2.5)$$

where P is the pressure, ρ is the density of the gas, $\gamma = \dfrac{c_p}{c_V}$ is the ratio of the specific heat at constant pressure (c_p) to the specific heat at constant volume (c_V), M is the molecular weight, R is the gas constant, and T is the absolute temperature.

The velocity of sound in liquids depends on the compressibility and density of the medium and is calculated from the formula

$$c = \sqrt{\frac{1}{\beta_{ad}\rho}} = \sqrt{\frac{\gamma}{\beta_{is}\rho}} \qquad (2.2.6)$$

where β is the compressibility,

$$\beta = -\frac{1}{V}\frac{dV}{dP} \qquad (2.2.7)$$

that is, β is the relative change in volume when the pressure changes by dP; and β_{ad} is the adiabatic compressibility, β_{is} is the isothermic compressibility, i.e., the compressibility at constant temperature.

In a slender solid rod the velocity of longitudinal waves is

$$c = \sqrt{\frac{E}{\rho}} \qquad (2.2.8)$$

where E is Young's modulus and ρ is the density of the solid.

In a rod where the cross-sectional dimensions are large in comparison with the wavelength (or in a solid of large dimensions), the velocity of sound will not be determined by Young's modulus, but by the so-called bulk modulus. For the same material the latter slightly exceeds Young's modulus.

The velocity of ultrasound in air is 344 m/sec at room temperature $(20^0 C)$.

The velocity of sound in a liquid is generally greater than in a gas under the same conditions. The velocity of ultrasonic waves in a liquid diminishes with increase in temperature. Water is an exception. The velocity of ultrasound in water increases at first, reaches a maximum at a temperature close to $80^0 C$, and then diminishes with further increase in temperature.

The velocity of ultrasonic waves in solids is greater than in gases and liquids. For instance, the velocity of sound in nickel is 5000 m/sec, and in iron 5850 m/sec. In heavy and inelastic metals (lead, for instance) the velocity of sound is 2169 m/sec.

For soft biological tissues (muscle, fat, nerves, liver), the velocity of ultrasound is 1490-1610 m/sec, while for bone tissue it is 3300-3380 m/sec.

As has been noted by Kinsler and others (1982), "theoretical prediction of the speed of sound for liquids is considerably more difficult than for (ideal) gases. However, it is possible to show theoretically that $\beta = \gamma \beta_T$ where β_T is the isothermal bulk modulus. Since no simple theory is available for predicting these variations, they must be measured experimentally and the resulting speed of sound expressed as a numerical (empirical) formula." Based on this point of view, it is essential that empirical relationships or point values based on experimentally determined values be used.

Important results obtained for propagation velocity as a function of temperature for tissues are presented in Figures (2.2.2 - 2.2.4)[4].
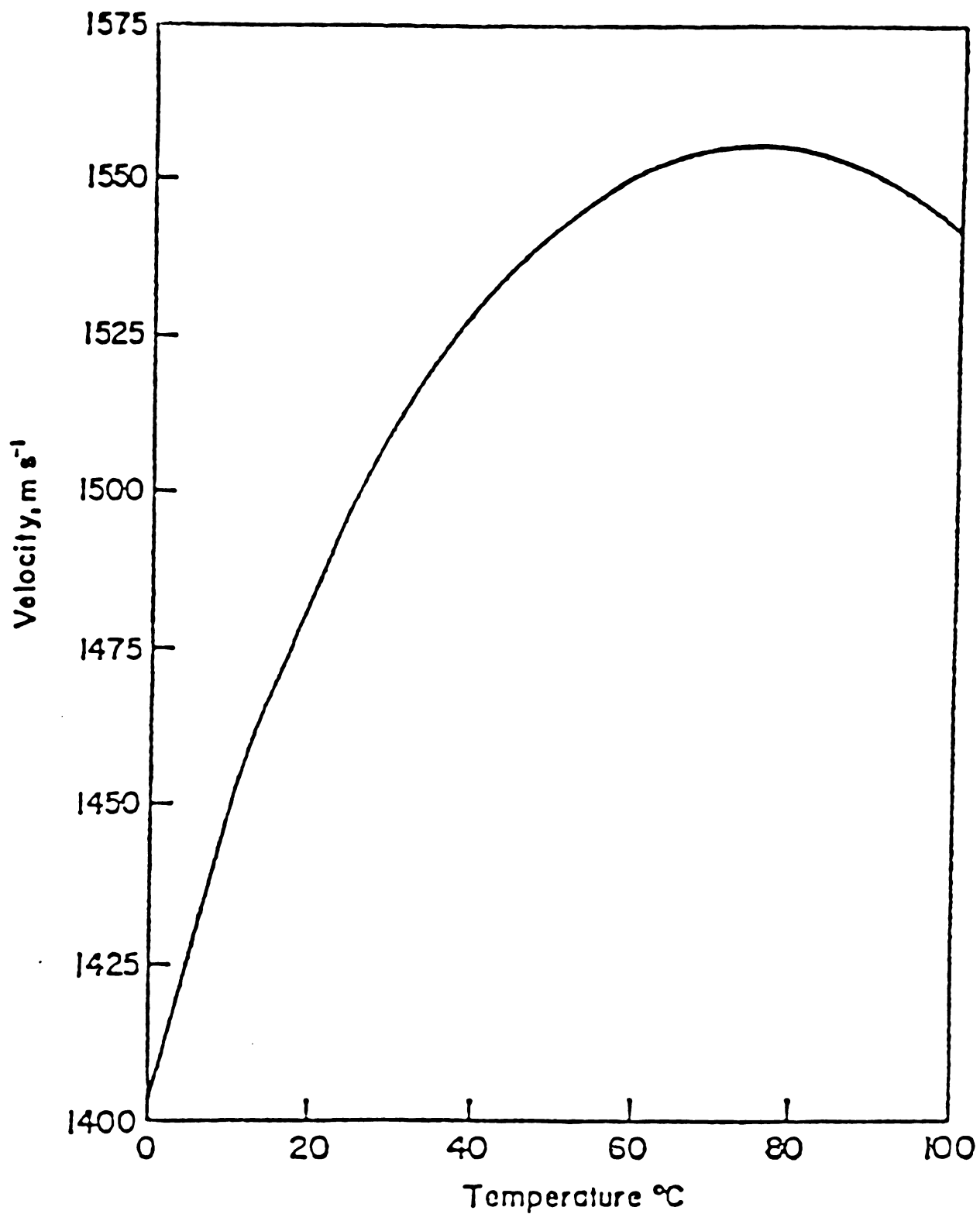
15

SPEED OF SOUND VS. TEMPERATURE
IN VIVO RUNS
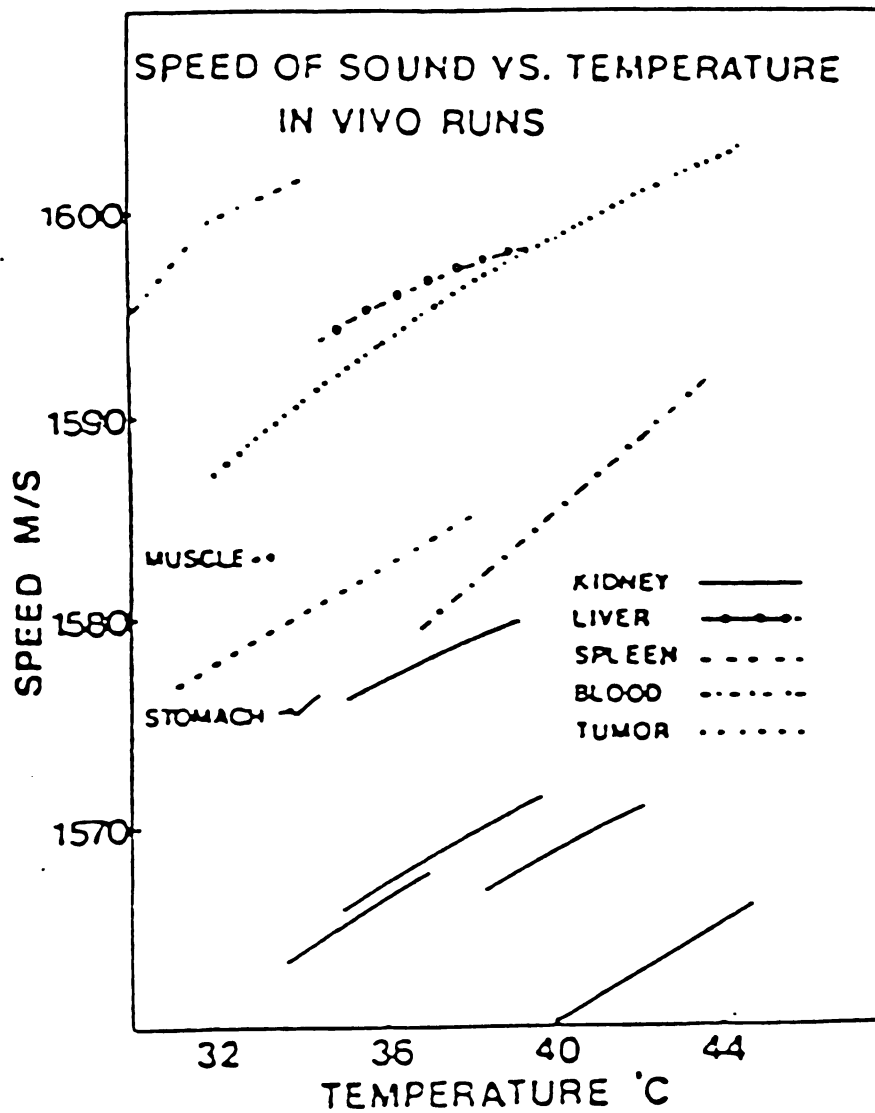
(Data from Nasoni, R. L., et al, 1980)

Figure 2.2.2 Speed of sound vs. temperature in-vivo runs.
(Data from Nasoni, R.L., et al, 1980)
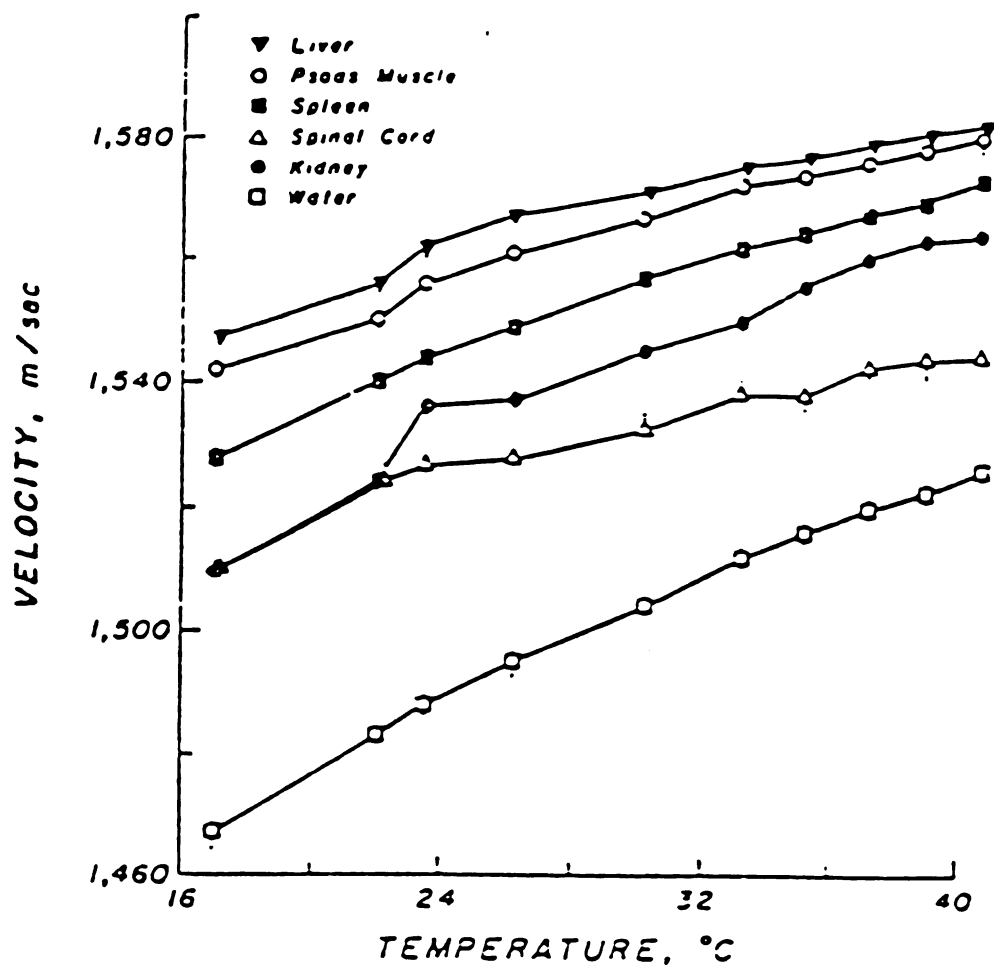
Figure 2.2.3 Variation of velocity of sound with temperature in various tissues. (Data from Johnson, S. A., et al, 1977)
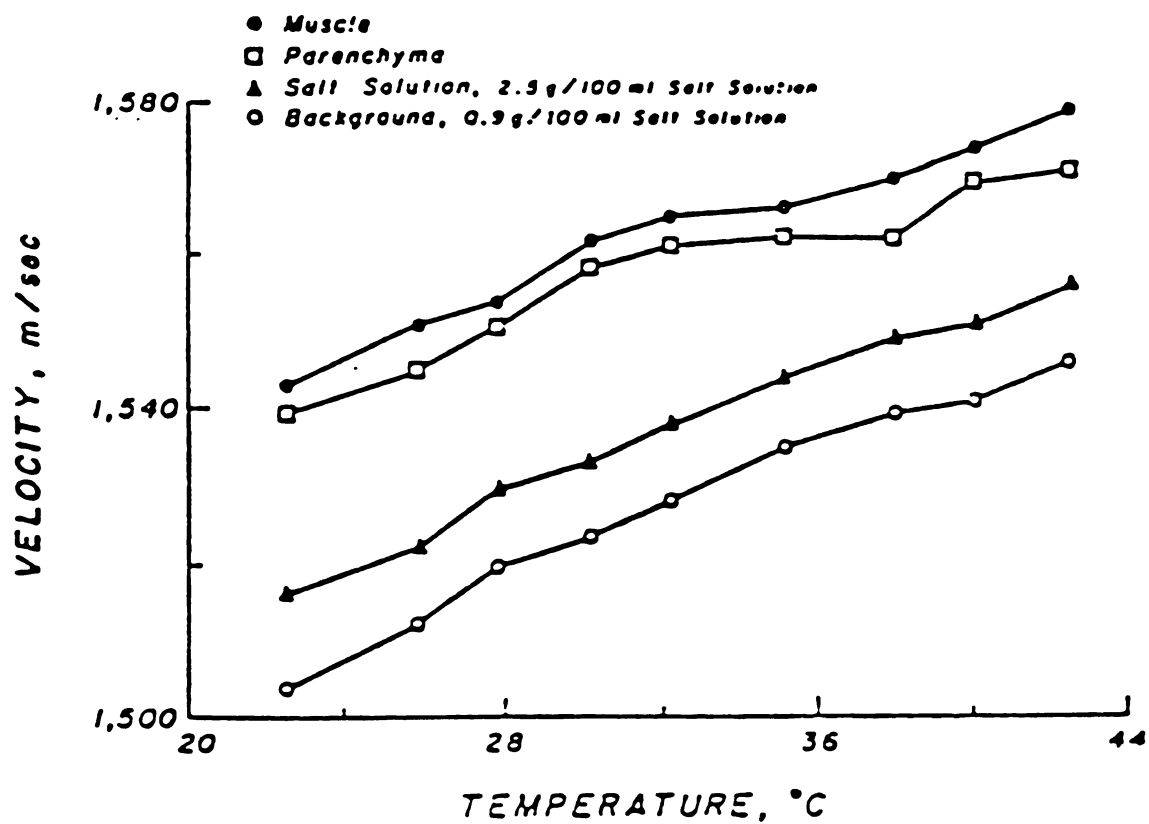
Figure 2.2.4 Variation of velocity of sound with temperature in breast tissues. (Data from Johnson, S. A., et al, 1977)

CHAPTER 3

Acoustic Consideration For Temperature Monitoring

It is useful to review the literature on the topic of acoustic temperature monitoring. Conclusions from either theoretical or experimental studies can be used in the design of our temperature monitoring system.

3.1 Ideal Step-Function Temperature Distribution Model

The ideal temperature for hyperthermia treatment is to have the tumor at a temperature of 42.5^0C or above and the surrounding healthy tissue at the normal temperature of 37^0C. The temperature distribution for this ideal situation was assumed using a step-function in some tissue studies. An example of the step-function distribution is shown in Figure (3.1.1).[1]

The step-function distribution lends itself readily to calculating temperature changes for non-invasive temperature monitoring because of its simplicity. With the lateral distance of the distribution, $2R$, specified by the rotation of the scanning focused ultrasound, an initial speed of ultrasound, c, through the tissue determined experimentally before the hyterthermia treatment or by using an assumed value, the rise in temperature can be determined from the change in the propagation velocity. The following equation can be used :

$$\Delta c = \frac{2R}{t_1 + \Delta\phi/\omega_d} - c_1 \qquad (3.1.1)$$

where $2R$ - outside diameter of the area of scanning focused ultrasound.

t_1 - initial propagation time across the distance $2R$.

$\Delta\phi$ - measured phase shift in radians.

ω_d - angular frequency of the diagnostic beam.

c_1 - the initial propagation velocity over the distance $2R_2$.

To determine the temperature change by using above equation, the relationship between the propagation velocity and temperature must be known.
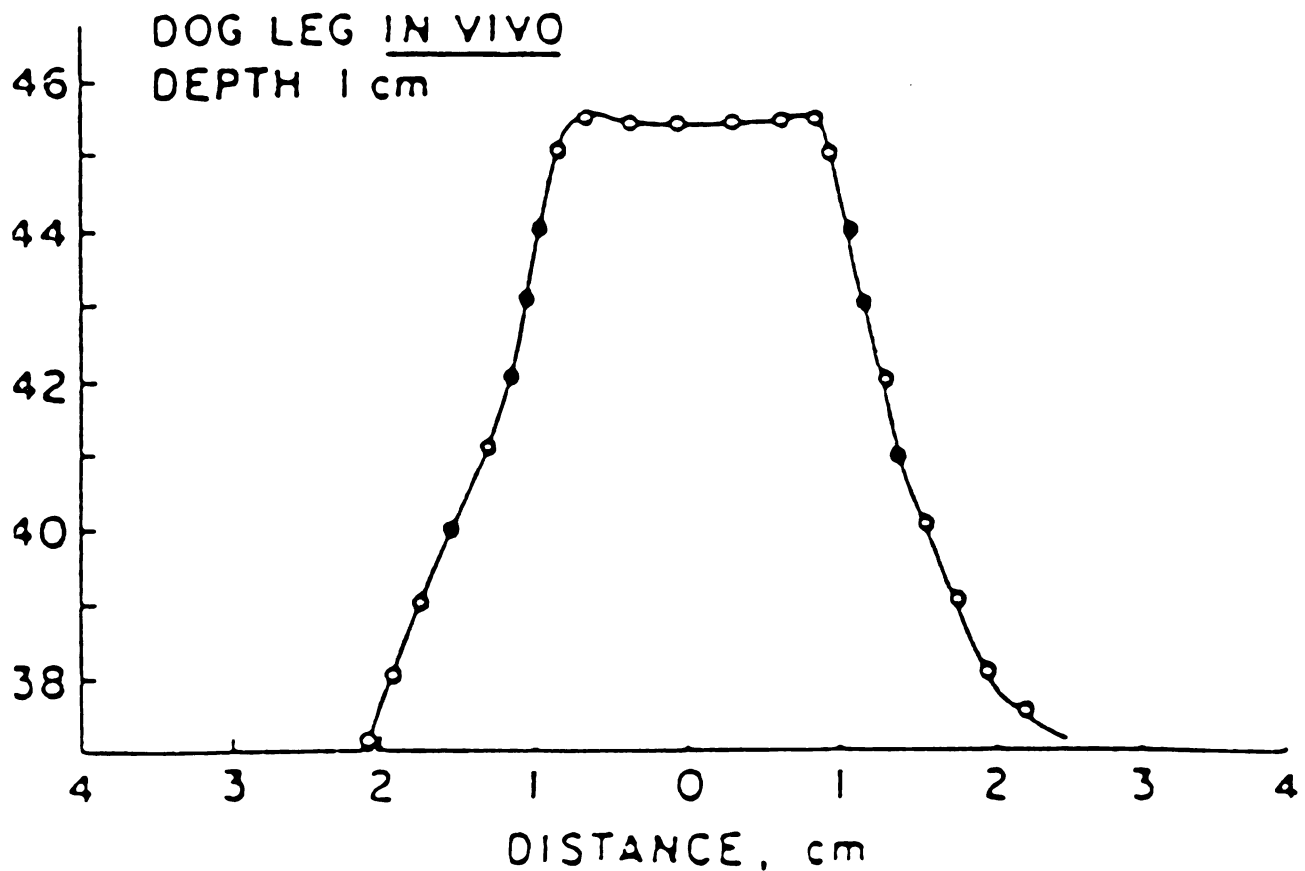
Figure 3.1.1 The above temperature profile, which closely resembles a step-function, is the simplest model from which many calculations for non-invasive temperature monitoring are derived. The most important of these calculations includes the determination of the required system accuracy.

3.2 Effect of Realistic Temperature Distribution

If the step-function model for the temperature profile were precise, then the change in propagation velocity could be used to determine the temperature rise directly and would involve ultrasonic scanning in one direction only. Since this is not the case, the next important consideration in the analysis of monitoring temperature distributions by acoustic means is then the examination of the temperature distribution as it deviates from a step-function. In fact, such an ideal temperature distribution is not possible because the heat flux $-k(\frac{\partial T}{\partial n})$ would be discontinuous at the boundaries. That is, the prescribed temperature distribution would be nondifferentiable at the boundaries and thus could not exist. This is illustrated by noting the "smooth" edges of the temperature distribution in Figure (3.1.1).

For hyperthermia treatment, the actual temperature profiles are unfortunately not always approximated well by step-functions, due to variable blood flow through tumors, their irregular shapes, and possible inhomogeneities in the associated acoustic and heat transfer properties such as density, thermal capacitance and conductivity. Thus the average temperature across a temperature profile may not necessarily correspond to the maximum temperature as is the case with a step-function-like distribution. Knowledge of the maximum and average temperatures is important in the treatment of

tumors by hyperthermia because of the known variable response of tissues to thermal doses. This effect is best illustrated by the results of a study done by Lele (1977) [5] shown in Figure (3.2.1). These results are also used in the formation of the protocol for treatment of tumors by focused ultrasound. As a consequence of these facts, it is useful to determine analytically the average temperature across a more realistic model of the temperature distribution as it relates to the maximum temperature in a step-function temperature profile. This analytical determination is useful because it indicates the deviation of the real temperature profile and can subsequently be used to evaluate the utility of one-dimensional ultrasonic scanning in this application.

As the conclusion of the study by Abramowitz, et al (1964) [6]. the ratio of the average temperature in the more realistic temperature profile and the average temperature across the ideal profile does not differ by much more than a factor of two. The range of values for $\bar{T}/T_{max}$ is 0.46 to 1.55. Since $\bar{T}/T_{max}$ does not differ by much more than a factor of two, the use of the step-function model to approximate the required system accuracies is appropriate. In addition, if a thermocouple is used to determine T_{max} while a tumor is being insonated with scanning focused ultrasound, the step-function model is still a good first approximation. The goal is, however, to use the change in propagation velocity across the insonation volume as a means to

calculate the maximum temperature directly. The conclusion is that if the temperature profile is indeed nearly a step-function, then the change in propagation velocity can indeed be used to calculate the maximum temperature directly given $c = f(T)$. But if the temperature profile evaluated is the more realistic one, $\bar{T}$, the average excess temperature across the distribution, can only be determined from the change in propagation velocity if:

(1) $c = f(T)$ is known and

(2) $c = f(T)$ is linear over the temperature range investigated.

The value $\bar{T}$, if determined, does not give as much information concerning the temperature profile in the realistic model as the value $T_{\max}$ does in the step-function model. This fact coupled with the third condition above are the major obstacles which limit the temperature profile information obtained by ultrasonic scanning in one-directin only.
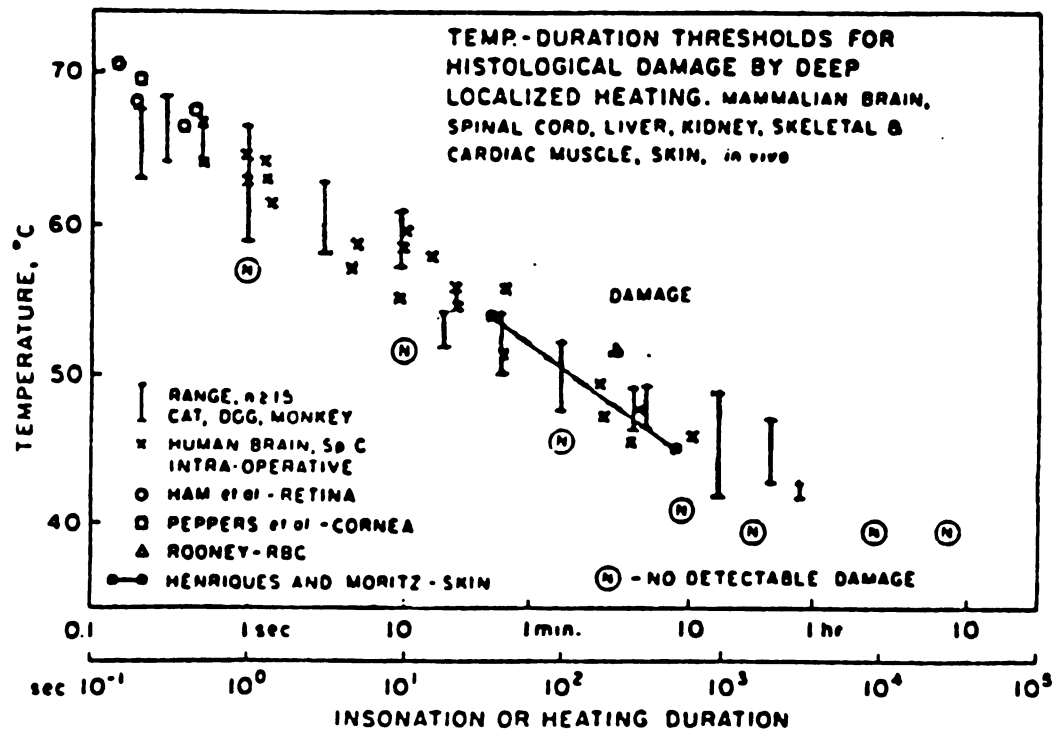
(Data from Lele, 1977)

Figure 3.2.1   Temperature - Duration threshold for histological damage by deep localized heating (Mammalian brain, spinal cord, liver, kidney, skeletal and cardiac muscle, skin).

3.3 Effect of the Nonlinear Relationship Between Temperature and Velocity

Another complication is the fact that many equations relating propagation velocity to temperature are nonlinear. The influence of this nonlinearity is best illustrated by examining a simplified model, which exists for the temperature distributions, for the empirical relationships between propagation velocity and temperature.

To demonstrate this point, consider a simple nonuniform temperature distribution as shown in Figure (3.3.1.a). Note that the average excess temperature through the distribution is $\bar{T}$. The approximate relationship between c and T is given in Figure (3.3.1.b). Figure (3.3.1.d) is obtained by switching the axes of Figure (3.3.1.a) and Figure (3.3.1.b). The estimate of the average temperature across the distribution is made and is compared to the average velocity. The simple result of the nonlinearity is that $\bar{c} \neq \overline{f(T)}$ although $c = f(T)$ for nonuniform distributions. (The bar notation above the variables represents the average value of that variable over the distribution). This is a very important point that does not seem to have been stressed in previous work done on the determination of $c = f(T)$ in tissues. In fact, in some studies a great deal of effort was expended using regression analysis to fit higher order polynomials with coefficients of three significant figures to the obtained data. It was assumed that the average temperature across a

nonuniform temperature profile could be used to determine the propagation velocity as a function of temperature even if this functional relationship were nonlinear. This error can further be illustrated analytically. Consider the functional notation for the temperature distribution and propagation velocity as a function of temperature given below:

(1) $T = g(x)$ is the temperature distribution.

(2) $c = f(T)$ is the propagation velocity as a function of temperature (non-linear).

The current average velocity over the temperature distribution from a to b is:

$$\frac{1}{b-a} \int_a^b f[g(x)]dx \qquad (3.3.1)$$

and this is correct average velocity provided that $c = f(T)$ is known.

If c has a linear relationship to T, i.e.,

$$c = A_1 T + A_2 \qquad (3.3.2)$$

where A_1 and A_2 are constant, then the average velocity may also be obtained from

$$f[\frac{1}{b-a} \int_a^b g(x)\, dx\,]. \qquad (3.3.3)$$

The impact of the nonlinearity between c and T with regard to ultra-sonic non-invasive temperature monitoring is that when there exists a

nonuniform temperature distribution, the change in ultrasonic propagation velocity cannot be used to determine the average change in temperature across the temperature profile unless

(1) the temperature distribution is ,in fact known to be uniform or

(2) the velocity distribution is determined by B-scan or C-scan. In either case, $c = f(T)$ must be known and the distribution prior to insonation must be uniform and known.
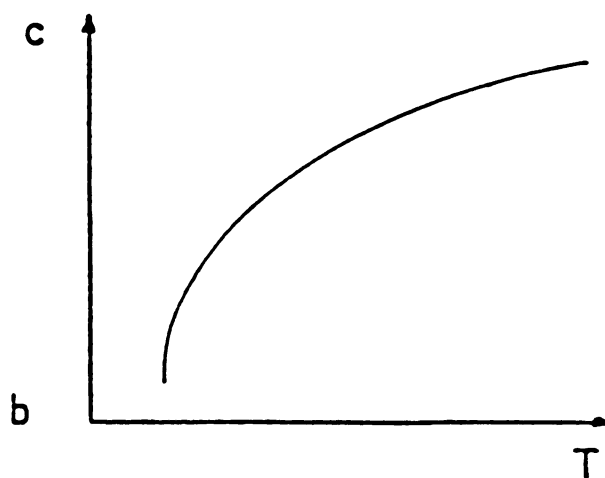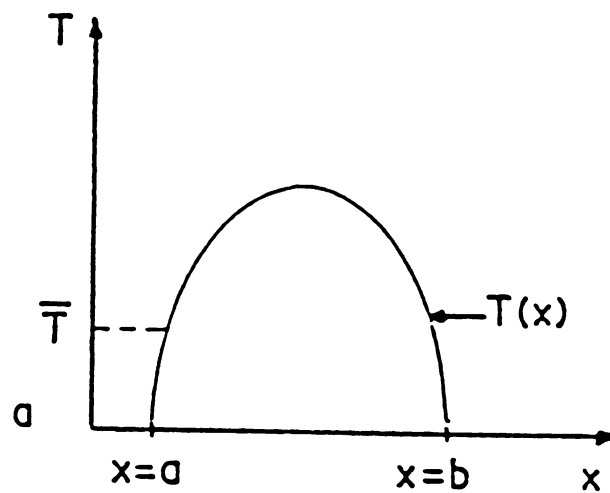
Figure 3.3.1 (a and b) Illustration of the problem associated with determining sound velocity as a function of temperature using the average temperature across a non-uniform temperature profile.
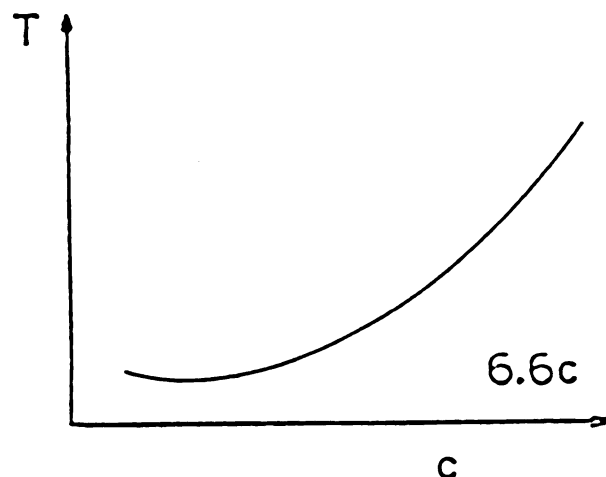
$$T = g(x)$$

$$c = f(T)$$

$$c(x) = f[\ g(x)\ ]$$

$$\bar{c} = \frac{1}{b-a} \int_a^b f[g(x)]dx \qquad (1)$$

$$\bar{c} \neq \frac{1}{b-a} f[\int_a^b g(x)dx] \qquad (2)$$
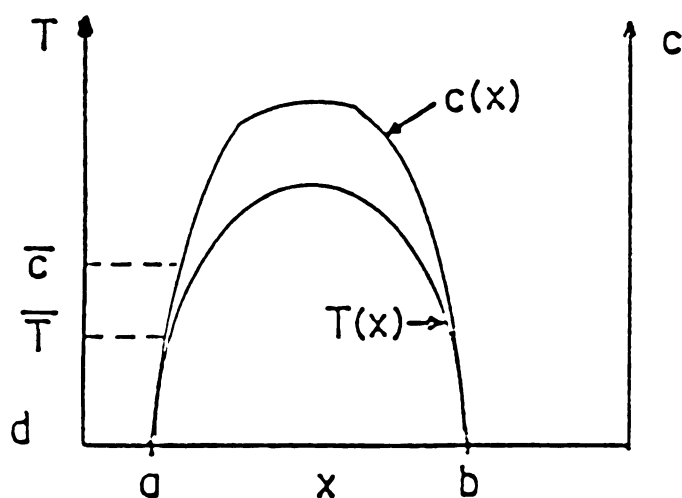
Figure 3.3.1 (c and d) Note: This is generally true for nonuniform temperature distributions and nonlinear relationships between c and T. In some limited cases (1)=(2), but (1) is the correct expression for $\bar{c}$ and (2) is not.

CHAPTER 4

Velocity Measurement Techniques

A variety of techniques have been developed for measuring ultrasound propagation velocity. Methods are used for either detecting temperature variation or determing characteristics of materials.

4.1 Review of Temperature Measurement

4.1.1 Interferometric techniques

Interferometric techniques are usually use continuous waves and only one transducer in a reflection mode. The velocity is measured by setting up a standing wave between the transducer and the reflector and varying the distance between the two, producing minima corresponding to integral numbers of half wavelengths. This technique relies on an accurate measurement of the distance between reflector and transducer and also on accurate measurement of the frequency. The velocity is then calculated from the known frequency and measured wavelength.

As noted by Wells (1977)[7], "the accuracy of the method depends on the parallelism of the opposite ends of the interferometer, and a high degree of mechanical precision is necessary."

Interferometric techniques suffer from several drawbacks when attempting to apply them to non-invasive thermometry. It is difficult to vary and measure, in living tissue, the change in distance associated with integral numbers of half wavelengths without altering the physical shape of the tissue. It does not seem to offer the advantages for non-invasive temperature monitoring during hyperthermia treatment.

4.1.2 Pulse-echo Overlap Technique

The pulse-echo overlap technique has been used widely [8] and has been analyzed extensively with regard to the effects of diffraction . The technique relies on measuring the period between a transmitted and received pulse either in the pulse-echo or pulse-transmit mode. The pulses are typically overlapped on an oscilloscope and the period measured with a counter. The period yields the propagation time and with known distance the propagation velocity can thus be determined.

The pulse-echo overlap method can be implemented by analog or digital instrumentation. In either case, the echoes must have similar waveforms so that corresponding features can be readily identified and brought into coincidence (i.e., overlapped). The method suffers when pulse-echo signals are weak or distorted by attenuation or other factors that render them unsuitable for the overlap approach.

4.1.3 The Phase-slope Method

As noted by D.R.Hull (1985)[9], with the phase-slope method, time between echoes is found by use of phase spectra of echo waveforms. After the echoes are digitized, a Fourier transform of each is obtained by a discrete FFT algorithm. The amplitude and continuous phase spectra for a pair of typical echoes are illustrated in Figure (4.1.1).

After Fourier transformation, both the amplitude and phase spectra are used to define a central zone within the frequency domain. For example, this zone may consist of only a narrow range near the center frequency or a frequency range for which the amplitude exceeds some fraction of the peak value, and/ or the zone may consist only of the frequency range for which the phase spectrum is linear. These restrictions eliminate the low and high frequency extremes where the signal-to-noise ratio is low.

The group velocity is given by

$$U(f) = \frac{2\pi(2s)}{\frac{d\theta}{df} - W} \qquad (4.1.1)$$

where f is frequency, θ is phase angle in radians, and W is the time delay between echo windows. In-window time delays for each echo can be calculated by setting $W = 0$ and solving for $T(f) = (d\theta/df)/(2\pi)$. Assume the phase spectra are linear functions of frequency in the central zone, their slopes are constants, $M = \frac{d\theta}{df}$, and the in-window time delays are $T_1 = \frac{M_1}{2\pi}$

for echo B1 and $T_2 = \frac{M_2}{2\pi}$ for echo B2. The total time delay is

$T = W + (T_2 - T_1)$. (Figure 4.1.2)

The frequency domain phase-slope method eliminates problems encountered in the time domain, e.g., the need to account for echo inversions. In addition, it provides convenient criteria for selecting an appropriate frequency range in cases where the major portion of the phase spectra of the echoes are mutually linear. Generally, for nonlinear dispersive cases, the phase-slope method can determine group velocities as functions of frequency. However, if signal-to-noise ratio is low, as was the case for the composite samples, poor results are obtained.

VOLTAGE, V

AMPLITUDE, N=115

F,
(s
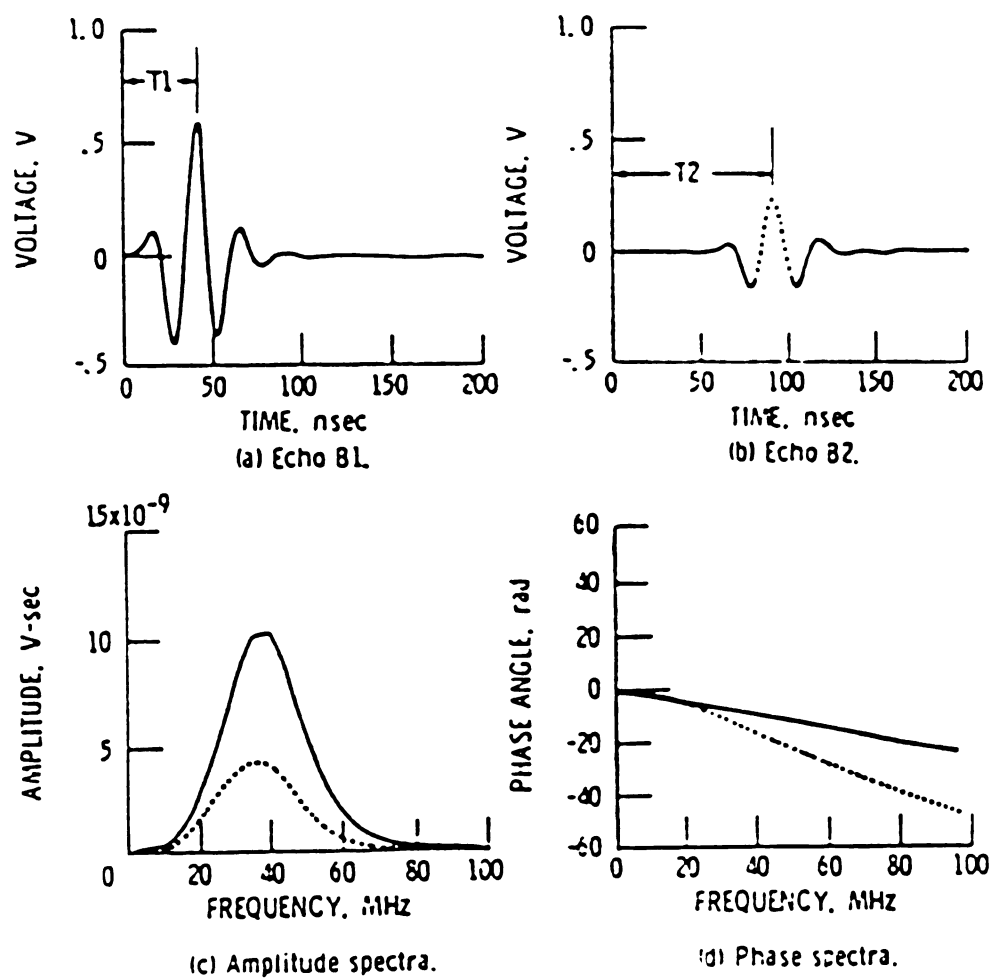
Figure 4.1.1 The Phase-slope Method. Typical back-surface echoes, B1 (solid) and B2 (dotted), and their amplitude and phase spectra.
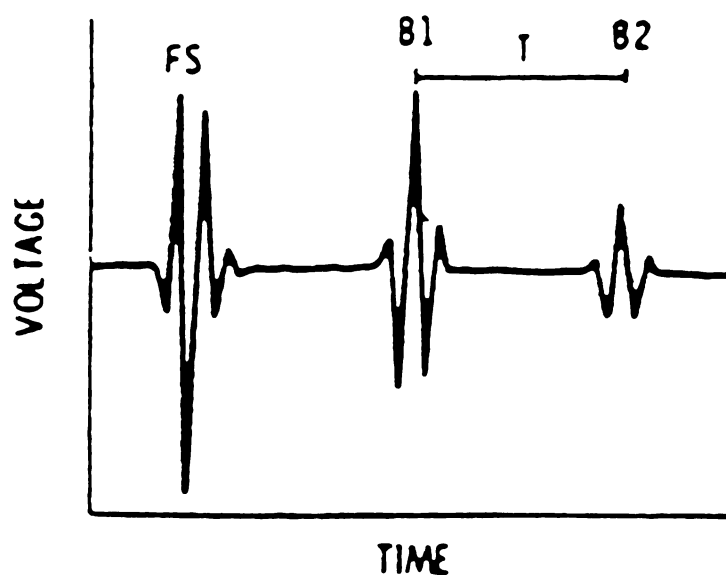
Time domain trace of principle echoes.

Figure 4.1.2.a   Time domain trace of principle echoes. Echo FS is returned by the front surface of specimen, and B1 and B2 are successive echoes returned by the back surface. Time T is the round-trip time delay between echoes B1 and B2.
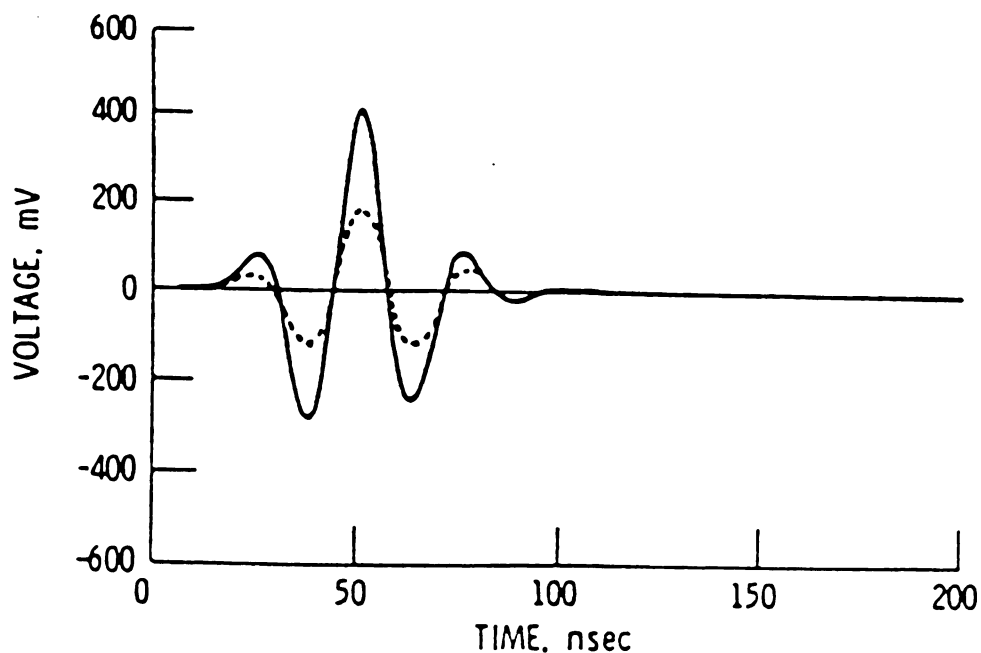
Figure 4.1.2.b   Result of digital overlap method for determining delay between echoes $B1$ (solid) and $B2$ (dotted) using echoes.

4.1.4 Cross-correlation Method

Unlike the overlap or phase-slope methods, the digital cross-correlation method does not require explicit criteria for accepting or rejecting specific features in echoes affected by distortion or signal-to-noise ratios.

The method is illustrated in Figure (4.1.3) , which shows the normalized cross-correlation function for three cases of echo positions. The cross-correlation function of two time domain signals is obtained by conjugate multiplication using their Fourier transforms in the frequency domain and retransformation back to the time domain. The cross-correlation function possesses a maximum in the time domain. The displacement of this maximum relative to a zero reference gives the time interval C, which for the ideal case should equal $T2-T1$ as measured by the digital overlap method. Cross-correlation gives this quantity whether the echoes appear in the same or separate windows. If the echoes B1 and B2 are separately windowed, then $T=W+C$.

For the relatively simple and undistorted echoes of Figure (4.1.3), cross-correlation gives results similar to those obtained by the two previous methods. The validity of the cross-correlation method depends on the fact that the displacement of the maximum of the cross-correlation function equals the time delay between the two successive echoes.

The advantages of the cross-correlation method are apparent when the signal-to-noise ratio is low and/or random noise is superpositioned on the echoes. One of the properties of the cross-correlation function is that it is (statistically) weighted by dominant frequencies common to the waveforms being correlated. Therefore, it returns a group velocity within the frequency bandwidth of the signals analyzed.

(b) T1<T2.

(c) T1>T2.
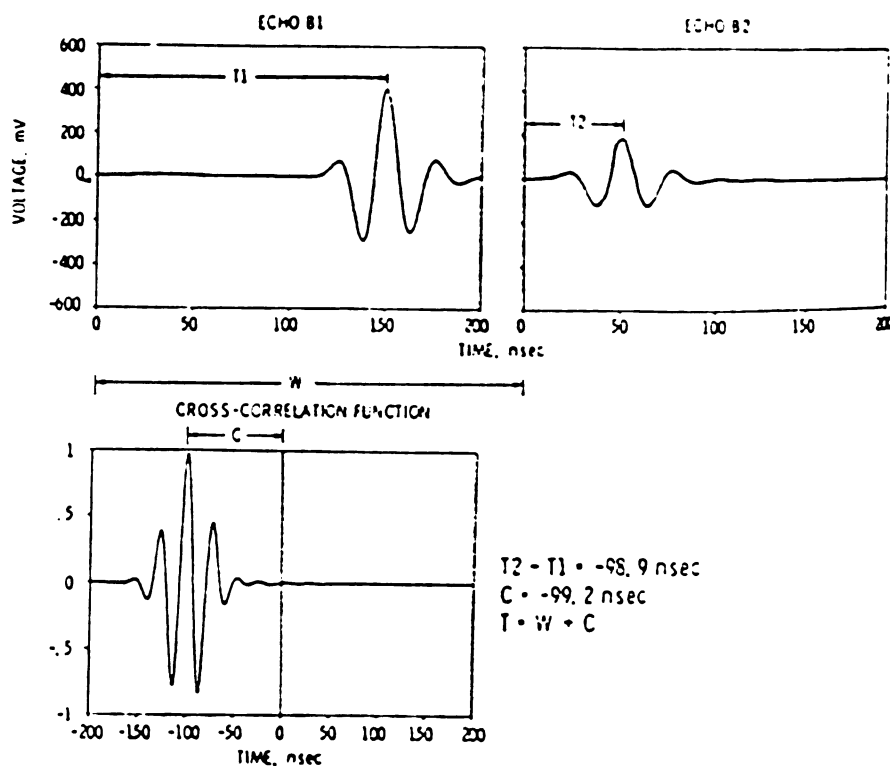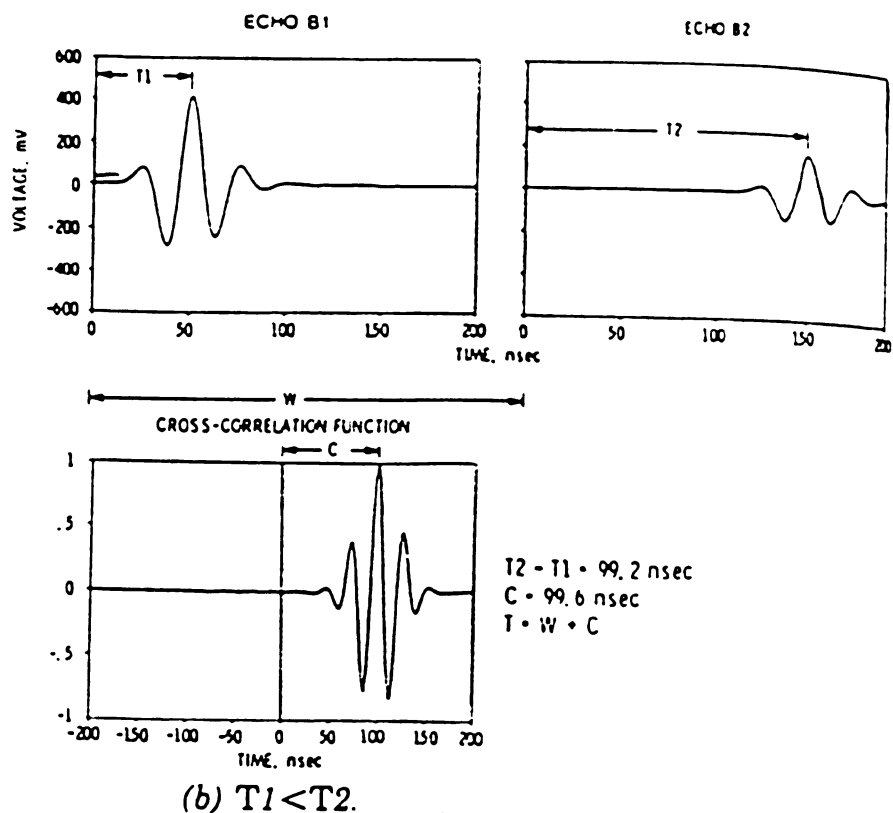
Figure 4.1.3 Result of generating the normalized cross-correlation function for two cases of echo positions. The displacement of the absolute maximum of the cross-correlation function relative to the zero reference guves the time delay C. For these ideal echoes, C was equal to T2-T1 as measured by digital overlap within the data-sampling interval error of 0.4 ns.

4.1.5 Acoustic phase shift technique

An acoustic phase shift technique for non-invasive measurement of temperature changes in tissues was developed by B.J.Davis and P. Lele (1985).[10]

The phase shift of an interrogating pulsed ultrasonic sine wave (diagnostic beam) is used to measure changes in its propagation velocity through the heated region corresponding to the temperature change. The system operation is in pulse-transmit mode, which use two transducers, for transmitting and receiving respectively. As shown in Figure (4.1.4), (4.1.5) and (4.1.6), the data recorder is triggered from the transmitting pulse and has a variable time delay which is held constant during and after the hyperthermia treatment. The change in propagation time is measured by determining the change in total delay time. The change in propagation velocity Δa and other known parameters is given by the following:

$$\Delta C = \frac{2R_2}{t_1 + \Delta t} - c_1 \qquad (4.1.2)$$

where t_1 is the initial propagation time, Δt is the change in propagation time, c_1 is initial propagation velocity over the distance $2R_2$, $2R_2$ is the distance over which the temperature rise occurs (insonation pattern diameter).
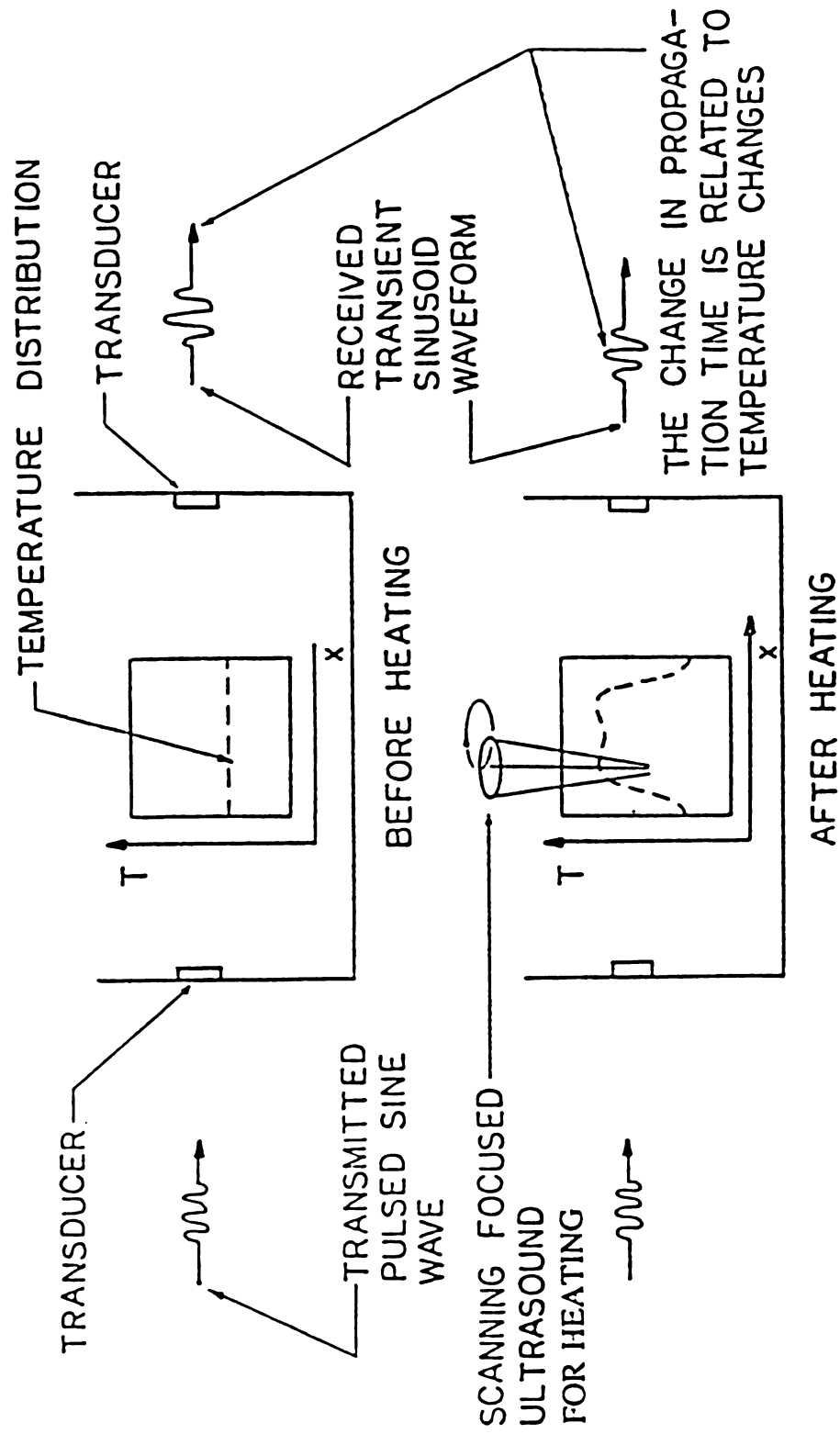
Figure 4.1.4 The concept of system operation for Phase Shift measurements.
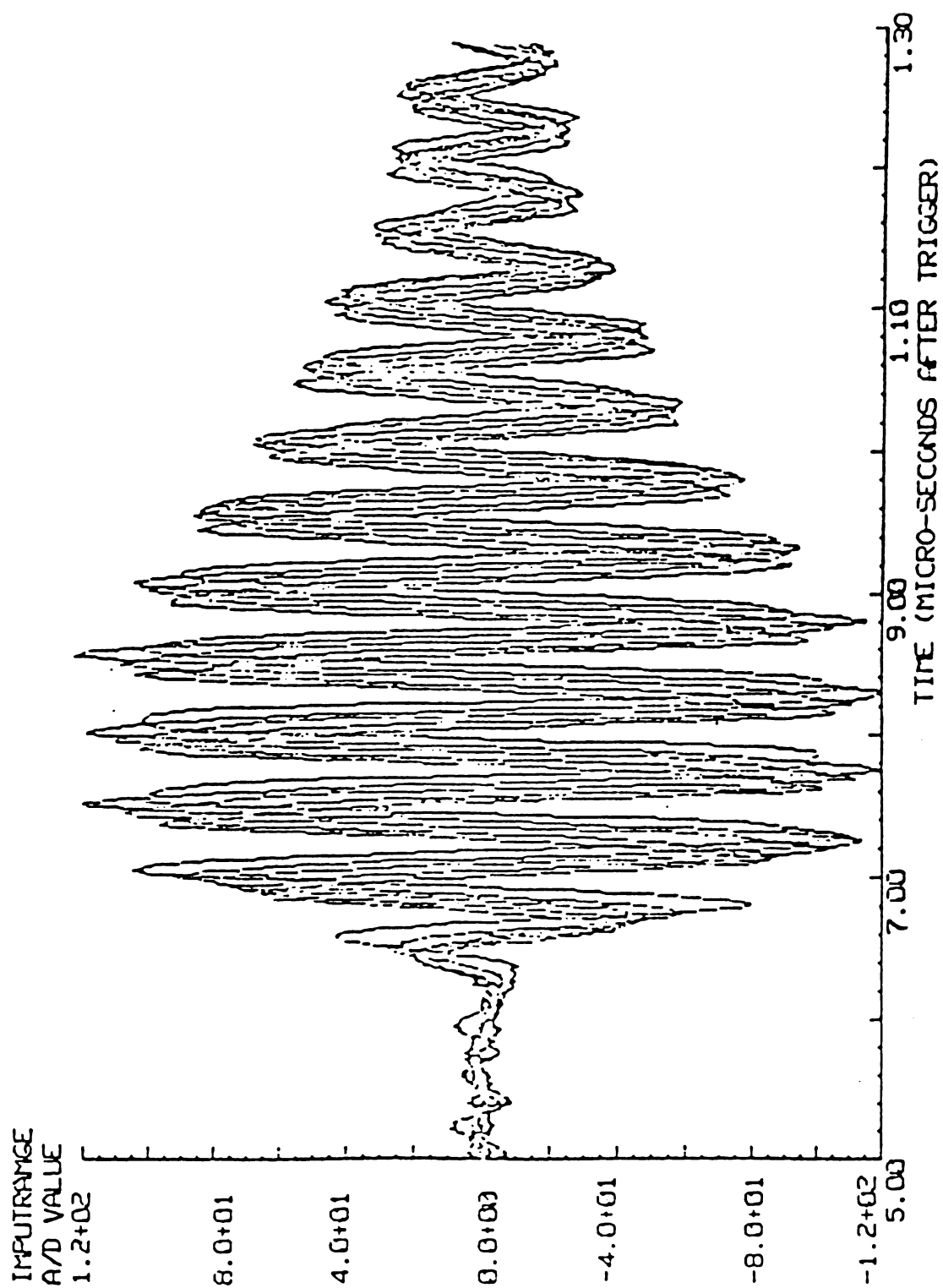
Figure 4.1.5 Phase Shift effect of five different waveforms from five different temperatures.
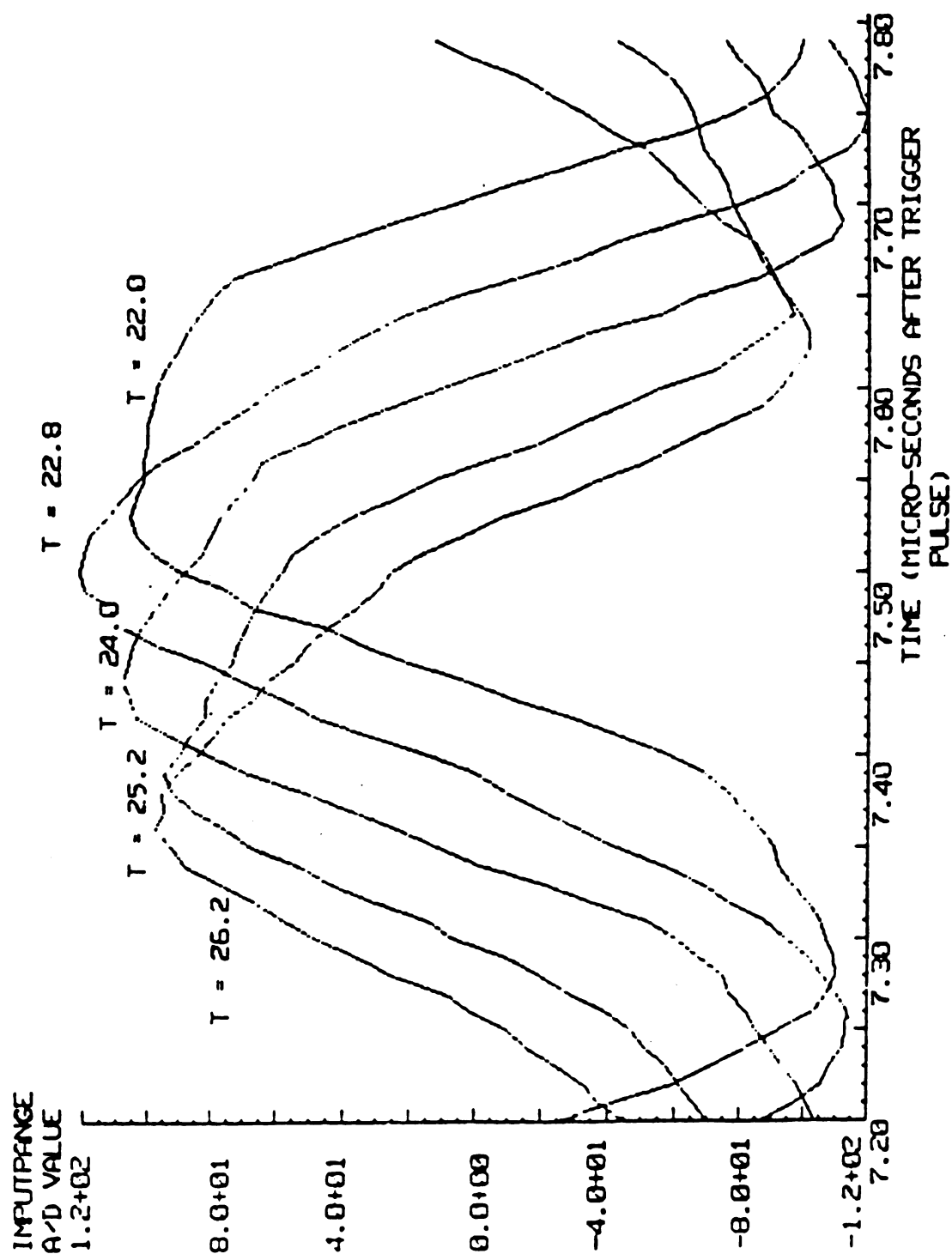
Figure 4.1.6 Acoustic Phase Shift with Temperature. (The above waveforms were recorded during simultaneous insonation with scanning focused ultrasound of muscle and liver tissue.)

4.1.6 Other Techniques

Greenleaf, Johnson, and co-workers [11] have shown that a reconstruction method similar to that used by X-ray reconstruction may be used to reconstruct the spatial variation of attenuation and refractive index in a special class of data collection geometries. The spatial distribution of the value of many measurable parameters may be determined by inverting the line integrals of a related acoustic variable along a set of refracted and/or reflected ray paths; in particular, the propagation time along a ray is the line integral of a specific function of acoustic refractive index.

Based on above theoretical approach, which indicates that high resolution reconstruction images may be obtained by accounting for the refracted or curved ray, a joint program between S.A.Johnson at the Mayo Clinic and D.A. Christensen at Utah resulted in experimental evidence that internal temperature distributions of static materials could be reconstructed with ultrasound techniques. An example of the reconstruction of the temperature of three water-filled balloons was demonstrated. The experimental configuration is shown in Figure (4.1.7).

Ultrasound reconstruction methods for determining temperature depend on theories developed for analysis of transmission data. These theories limit the use of the body, such as the breast, where reflection and absoption

effects are minimal. This technique also suffered from the inaccessibility of in-vivo experiments in medical applications.

A method used by Dunn and Fry (1961) to determine the acoustic velocity in the lung relied on determining the change in acoustic impedance, ρc, from the reflection at a lung-water interface.

Barlow and Yazgan (1965) determined the phase difference between a modulated r.f. pulse propagated through a known liquid path and the incident pulse reflected from a solid-liquid interface by cancelling each pulse separately against a continuous-wave signal which was adjustable in phase and amplitude. From two such measurements at slightly different frequency the total phase shift in the liquid is calculated and then related to the propagation velocity.

Figure 4.1.7.a   Ultrasound Computerized Tomography System.
(Data collection and control)

4.2 Temperature measurement technique in this research

The ultimate purpose of the temperature measurement system is for medical applications such as hyperthermia treatment. Such techniques as the interferometric technique and cross-correlation technique are often claimed as having a high degree of accuracy and precision. But these techniques are not well-suited for this application, because they require a relatively noise-free acoustic environment for their successful operation. Since transmission mode measurements suffer from the inaccessibility of in-vivo experiments, an alternative pulse-echo mode measurement has been chosen in this system.

The pulse-echo technique used here is also under the assumption that the speed of ultrasound as a function of temperature is given by an expression of the form:

$$V = V_0 + mT + qT^2 \qquad (4.2.1)$$

It has been observed that V_0 is not constant for all tissues, while m is nearly constant for all tissues from 37^0C to 44^0C; which is the temperature range in hyperthermia treatments. The parameter q is very small in this temperature range for most tissues thus the velocity is linearly proportional to the temperature T.

Acoustic velocity measurement techniques generally are able to meas-

ure changes in velocity much more accurately than absolute velocities. Consequently, with regard to non-invasive temperature measurement, a change in temperature is measured much easier than is the absolute temperature. This fact is particularly important if one considers that the temperature coefficient of velocity is fairly constant for most tissues, whereas absolute propagation velocity is known to vary. As a result, information regarding initial body temperatures prior to therapy is important in order to determine absolute temperature in tissues.

The temperature change is determined as follows:

$$V_{orig} = V_0 + m \; T_{orig}$$

and

$$V_{new} = V_0 + m \; T_{new}$$

are substracted to give:

$$T_{new} = T_{orig} + \frac{1}{m}[V_{new} - V_{orig}] \qquad (4.2.2)$$

where T, M, and V were defined previously and "new" refers to the new temperature to be measured and "orig" refers to the original known temperature. The value of "m" in the above equation could be assumed as the average for the representative tissues. It is concluded that the temperature change is also linearly proportional to the velocity change which can be measured by the ultrasound pulse-echo techniques outlined in this system. The basic arrangement of the system and its operations are discussed in

Chapters 5 and 6.
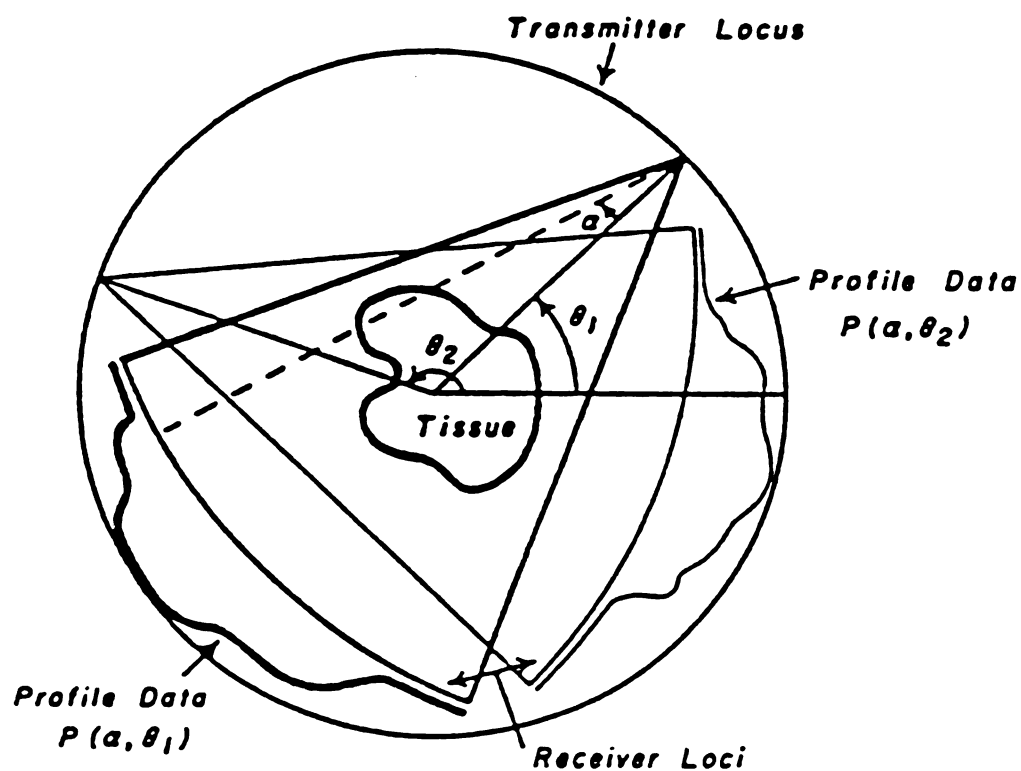
Figure 4.1.7.b   Data Collection Geometry For Ultrasonic computerized Tomography. (Geometry of two typical transmitter locations, dark and light lines. Note separated locus and centers of rotation of transmitter and receiving transducers).

CHAPTER 5

System Configuration and Operation

5.1 Hardware Description

In this project, both a non-intrusive temperature measurement system and an intrusive temperature measurement system were built for make comparison with each other. We used the intrusive method to verify the non-intrusive method where it is applicable.

5.1.1 Non-intrusive temperature measurement system

The ultrasonic scanning system used for non-intrusive temperature measurement is shown in Figure (5.1.1). The transducer is used for both ultrasound pulse transmitter and receiver. It is a long focused, piezo-electric transducer with 2.25 MHz resonance frequency. The pulse waveform is shown in Figure(5.1.2).

The stepping motor and its controller is used for 2-dimensional scanning. The scanning part uses two synchronous stepping motors and the scanning resolution is about 1 mm, and the scan area is about 128 mm. by 128 mm. By using 2-dimensional scanning, a temperature gradient (or distribution) can be obtained.

A panametrics 5050 Pulser is used as a pulse generator and echo receiver. The Receive/Transmit mode of the pulser is used in the system operation. For transmit, the pulser portion of the 5050 Pulser is controlled by the external trigger, which is generated by the RANGE -GATE . After exciting a pulse to the transducer, the 5050 Pulser switches to the receive mode . The receiver portion of the 5050 Pulser is a 40 dB amplifier, with a three position attenuation control, which allows the input signal to be attenuated prior to amplification. The receiver output is limited to 2 V_{p-p} which meets the requirement of the A/D converter.

The RANGE-GATE is a time-delay controller that controls the time delay between the external trigger pulse and the sampling enable signal. Because of the limited buffer size, which is 1024 bytes, it is useful to receive all of the echos from the specimen in the time interval of propagation from the transducer to the specimen. The delay time in sample time intervals can be anywhere from 1 to 255.

The sampling and A/D conversion board were specially designed for this temperature probing system. The system core is a TRW 1048 monolithic video A/D converter. It is capable of sampling at rates up to 20 MHz, which is sufficient to sample a signal up to 5 MHz. Dual clocks are used in this board, one at 14.667 MHz for sampling and conversion and the other at

100 KHz for transferring data from the A/D buffer to the system controller (Crommemco Z-2D micro-computer) memory through the S-100 bus. The reason of not using 20 MHz clock for the sampling rate is that the system is more reliable at the signal frequencies of interest which range from 0.5 MHz to 5 MHz.

The system controller is a Crommemco Z-2D micro-computer, in which programs are written in Z-80 assembly language. One of the testing modes is a one-shot mode, in which the transducer launches a pulse signal to specimen and receives multiple echos back from the specimen. After being digitized, all the echo data are stored into a data file by the computer. The data obtained from this mode can be used for determining the temperature coefficient for velocity by signal processing to be described in Chapter 6.

Another mode is the Scanning test, which produces the temperature profile of a specimen. The algorithm at each physical position is the same as that of the one-shot mode described above. A scanning motor control program lets data at every position within the scanning area be stored .

An IBM-PC computer is used for purposes of post-data processing and graphic display. An Emulation program has been used for interfacing the IBM-PC and the Crommemco Z-2D. The Emulation program handles the communication between the two computers through a RS-232 interface. We

can use the IBM-PC either as a terminal of the system controller to issue all the operation commands to the Crommemco Z-2d or as a data-processor to evaluate the velocity change which indicates the temperature change. After obtaining the scanning data file, a display of the results may be performed.

53
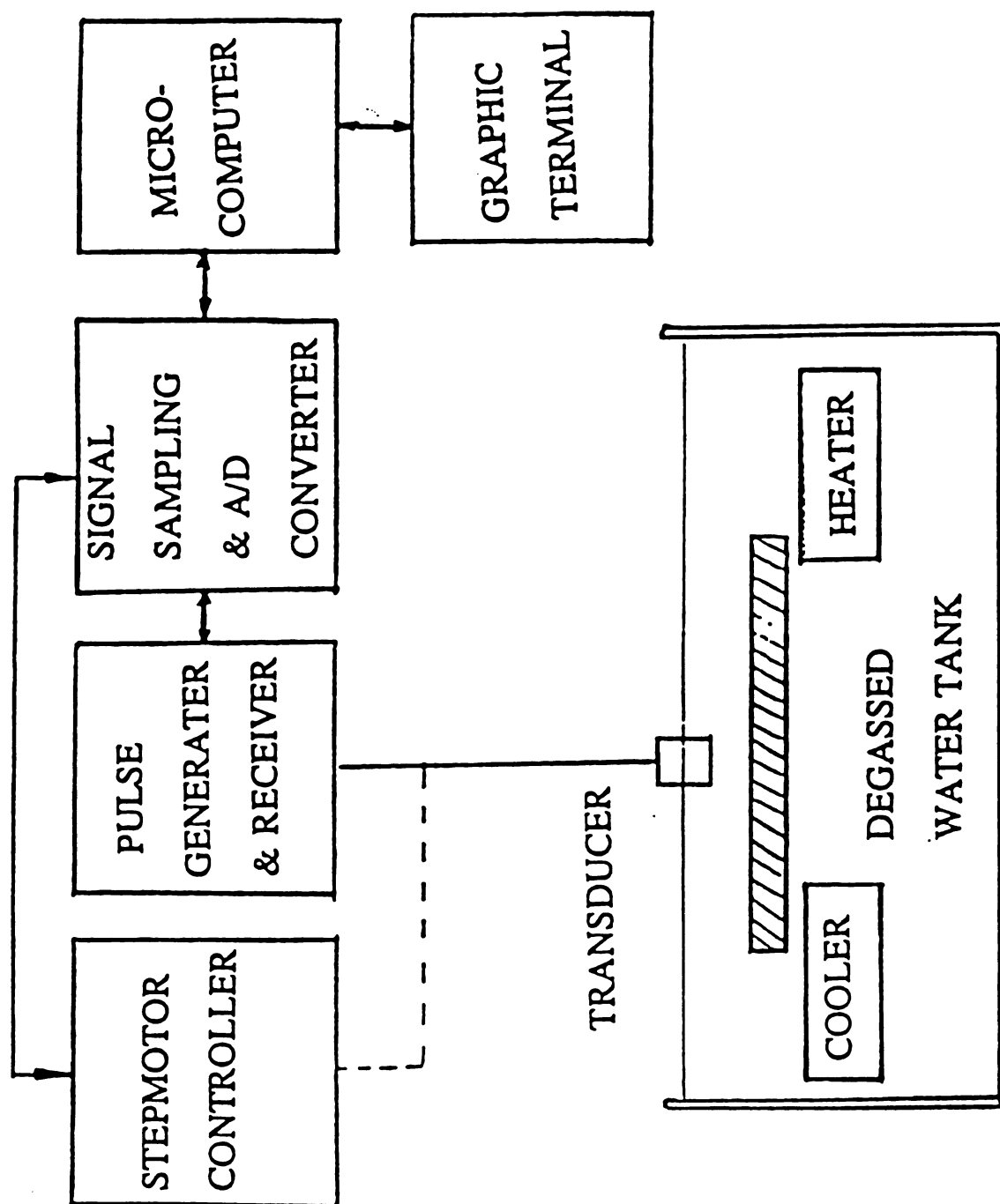
Figure 5.1.1   Non-intrusive temperature profile probing system.

Amplitude
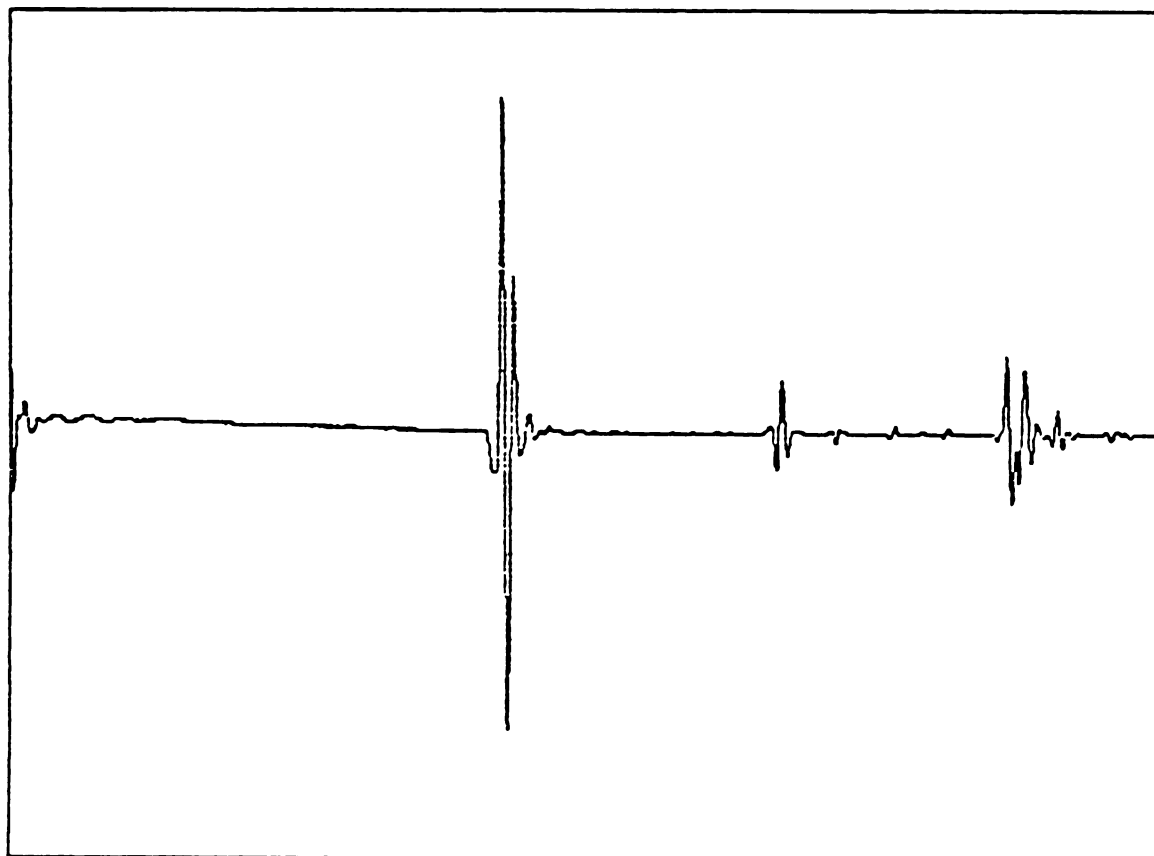
Time

Figure 5.1.2 The pulse waveform in time domain used in non-intrusive temperature measurement system.

5.1.2 Intrusive temperature measurement system

As a supplemental part of the project for comparison purpose, an intrusive temperature measurement system was built by using a fluoroptic thermometer, a commercial unit named Luxtron Model 750, which is a state-of-the-art thermometry system. The system is shown in Figure(5.1.3). This machine uses several optical fiber probes to measure different temperatures at the same time. The probe has temperature-sensitive phosphor material coated to its tip. In operation, the phosphor material is excited by a xenon flash. The induced flourescence starts decaying with time. The rate of decay is temperature dependent. By evaluating the decay rate, temperature can be measured with high precision (within a fraction of a degree) [15]. The temperature read out can be displayed on the front panel and also can be transmitted to a computer for post-processing.

Instead of using an ultrasound transducer and the Pulse transmitter/receiver, the Luxtron model 750 was connected directly to the system controller- Crommemco Z-2D with RS-232 serial ports. The temperature data read by the probe are transmitted to the system controller and saved for later processing.

In operation, a probe is moved by the scanner to make a 2-dimensional scan and obtain the temperature distribution data within the scanning area.

The system controller stores the data and then send it to an IBM-PC for 3-dimensional display.

A program was developed to make the Luxtron model 750 totally remote control, including the setting of all operation modes and parameters.
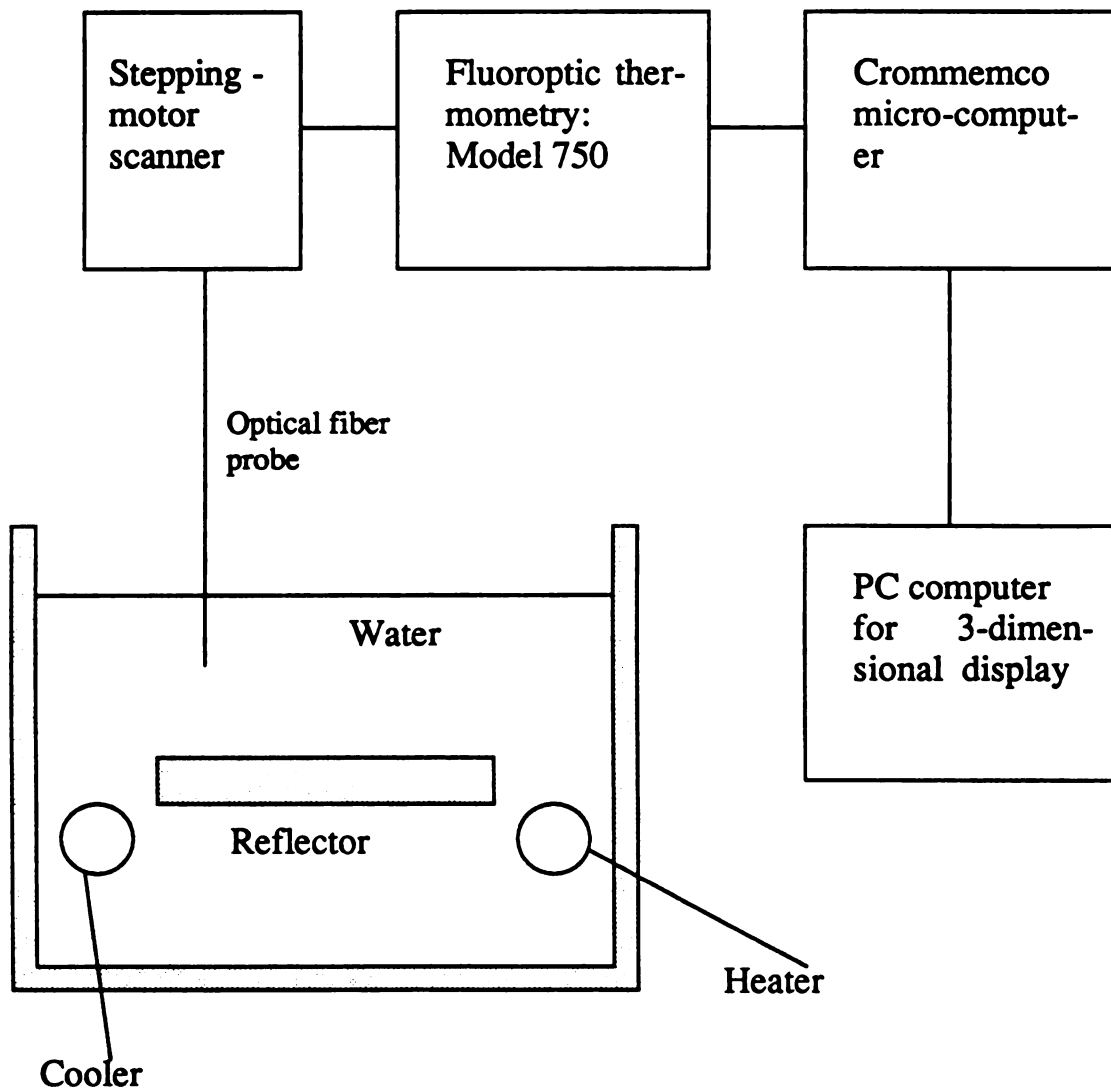
Figure 5.1.3   Block diagram of invasive temperature measurement
system

5.2 Software Description

The software used in this system are classified into two groups. It is convenient, for purposes of description, to consider the ultrasonic temperature measurement system as two distinct parts, one is scanning and data aquisition, the other is data processing and imaging.

The main flow charts of the scanning and data aquisition programs are shown in Figure (5.2.1). Note that each data record has three dimensional location information, say X, Y and Z. From the data stored on disk it is possible to extract the X and Y co-ordinates of each measurement point, and the Z co-ordinate as a boundary location. The Z co-ordinate is actually measured in terms of the time it takes the ultrasound to reach a boundary in the specimen and reflect back and, if the distance from the boundary to the transducer is relatively constant, this is proportional to the sound velocity. Thus, the comparison of time change will be converted to the velocity change and then mapped to the temperature change if the relationship of velocity and temperature is known.

In the group of data processing and imaging software the program for processing one-shot data, basically doing correlation and averaging as shown in Figure (5.2.2), is used for getting rid of noise. Since the correlation calculation can distinguish the time difference between two signals which

are offset by one sampling point due to the triggering uncertainty, this noise can be deleted. The noise free, averaged signal can be then processed (autocorrelated)to find the time interval which provides an accurate measure of velocity .

After running the scanning and data aquisition program, the data file obtained is processed in a PC computer to get a three-dimensional image. The program can find the time interval between boundaries at each position. This data file can then be displayed as a temperature profile on a cross-section of the layered model.

The main data processing program is implemented in a PC computer to process the data file obtained from the scanning and data aquisition program, which has three dimensional boundary location information. This program is ideal for experimental models which have well defined boundaries. The program reads the source data file and choose a certain Y position to process the correspondant cross section for a B-scan image. The program reorganizes the data into groups on different layers. After user specified layers, the distances between the layers for every lateral position is calculated, and the results are stored into a new file, a layer distance file, which can represent the time interval between boundaries at each position. In applications, scanning will be done twice prior to and after the heating process which will produce two data files. The B-scan image of these two files will show the

time intervals between two layers for all scan positions and will indicate the

velocity change inside the experiment model. This B-scan image can be

interpreted as a temperature profile cross section. The flow chart for the

software is shown in Figure (5.2.3).
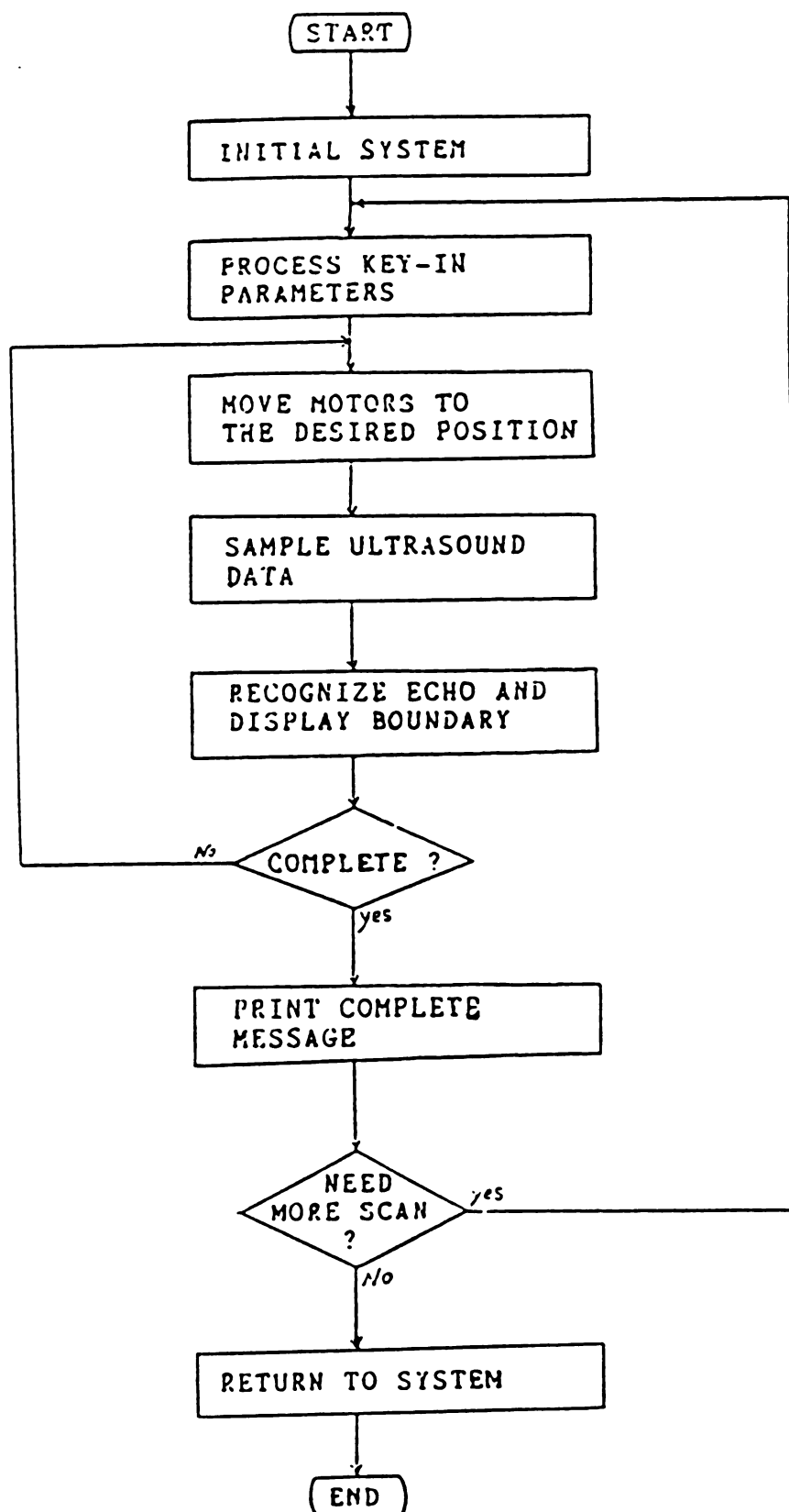
Figure 5.2.1 The main flow chart for the scanning and data aquisition program.

Input parameters;
1. the number of data files to be averaged.
2. correlation range

Read the first data file into an
array

Do loop: from n=2 to n=N

Read the nth data file;
Calculate correlation to get the difference
between two signals;
Two signals be averaged into one averaged
signal;

Store the averaged signal data into file.
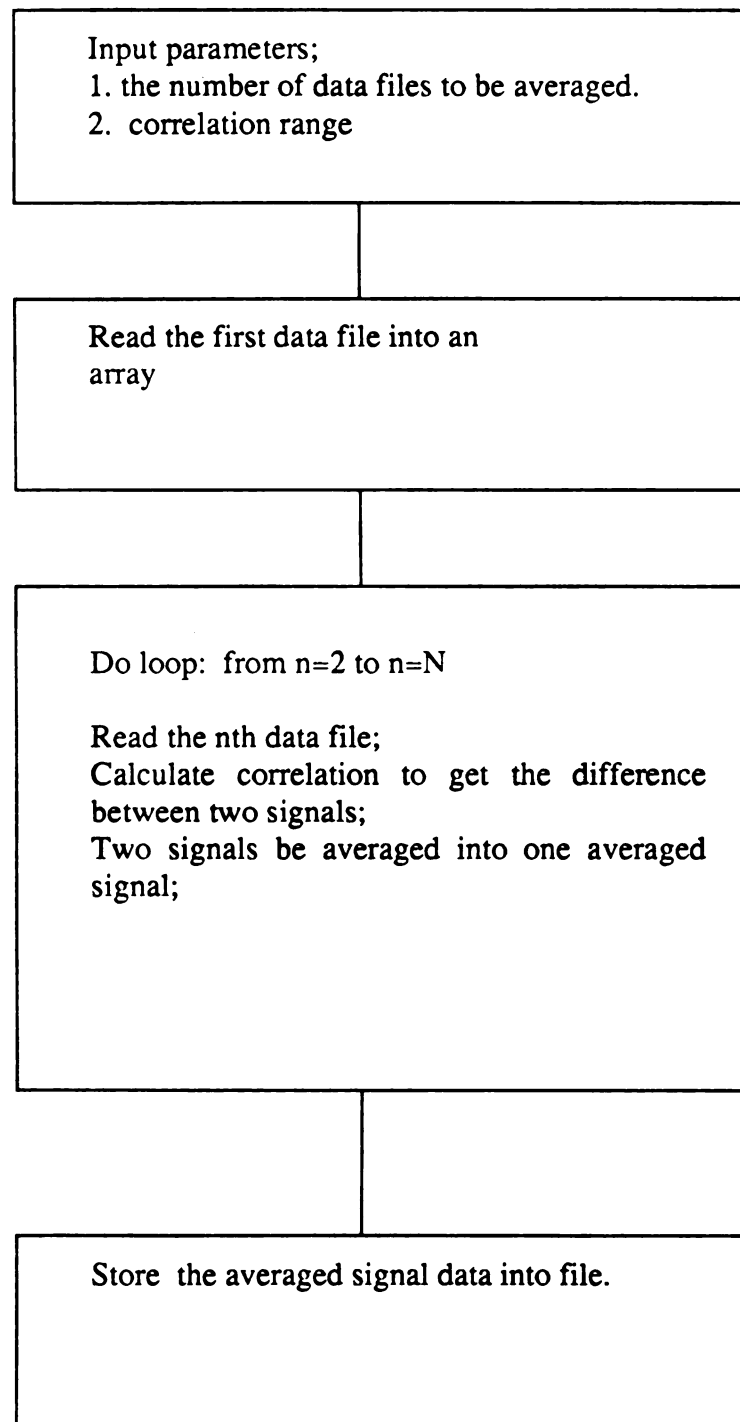
Figure 5.2.2   The flow chart of the data averaging program.

5.3 The System Operation

When using the non-intrusive ultrasonic temperature measurement system, a PC computer is used as a terminal to issue all the operation commands. Initially , an Emulation utility is run to set up the connection to the system controller, the Crommemco Z-2D, in order to manipulate the measurement operation through the terminal.

After setting the scan area parameters, which are X and Y axis range, step length, the sampling delay time and the echo signal detection threshold, the scanner translates the transducer over a specimen in a degassed water tank. A pulse wave is emmitted at each scan position by the 2.25 MHz transducer. Echos are received and are digitized to detect the boundaries by the data aquisition program, and only the boundary position value are stored. The data are stored in the format of (X,Y,Z). The change of boundary position in the pulse transmission and receiving path indicates the change of velocity. If we can get rid of other factor which could affect the boundary position, such as system uncertainty and the movement of the specimen, the boundary position shift can be mapped into a temperature change profile.

After the system controller completes the scanning, the data file is transferred to the PC for post data processing. The imaging software will construct an image of the three-dimensional data stored during the scanning

64

process and will project it onto a two-dimensional viewing screen.

```
                    ┌─────────────┐
                   (    Start      )
                    └─────────────┘
                           │
        ┌──────────────────────────────────────┐
        │      Do loop:  read data from files.   │
        └──────────────────────────────────────┘
                           │
        ┌──────────────────────────────────────┐
        │   Choose a cross section to do B-scan image.  │
        └──────────────────────────────────────┘
                           │
        ┌──────────────────────────────────────┐
        │      Regroup the data according to layers.   │
        └──────────────────────────────────────┘
                           │
        ┌──────────────────────────────────────┐
        │   List data according to layers or make hard copy .  │
        └──────────────────────────────────────┘
                           │
        ┌──────────────────────────────────────┐
        │      Input parameters for choosing two layers.   │
        └──────────────────────────────────────┘
                           │
        ┌──────────────────────────────────────┐
        │   Count the distance between the two layers.   │
        └──────────────────────────────────────┘
                           │
        ┌──────────────────────────────────────┐
        │ Store data into a file to be displayed as a B-scan image.  │
        └──────────────────────────────────────┘
                           │
                    ┌─────────────┐
                   (    End       )
                    └─────────────┘
```
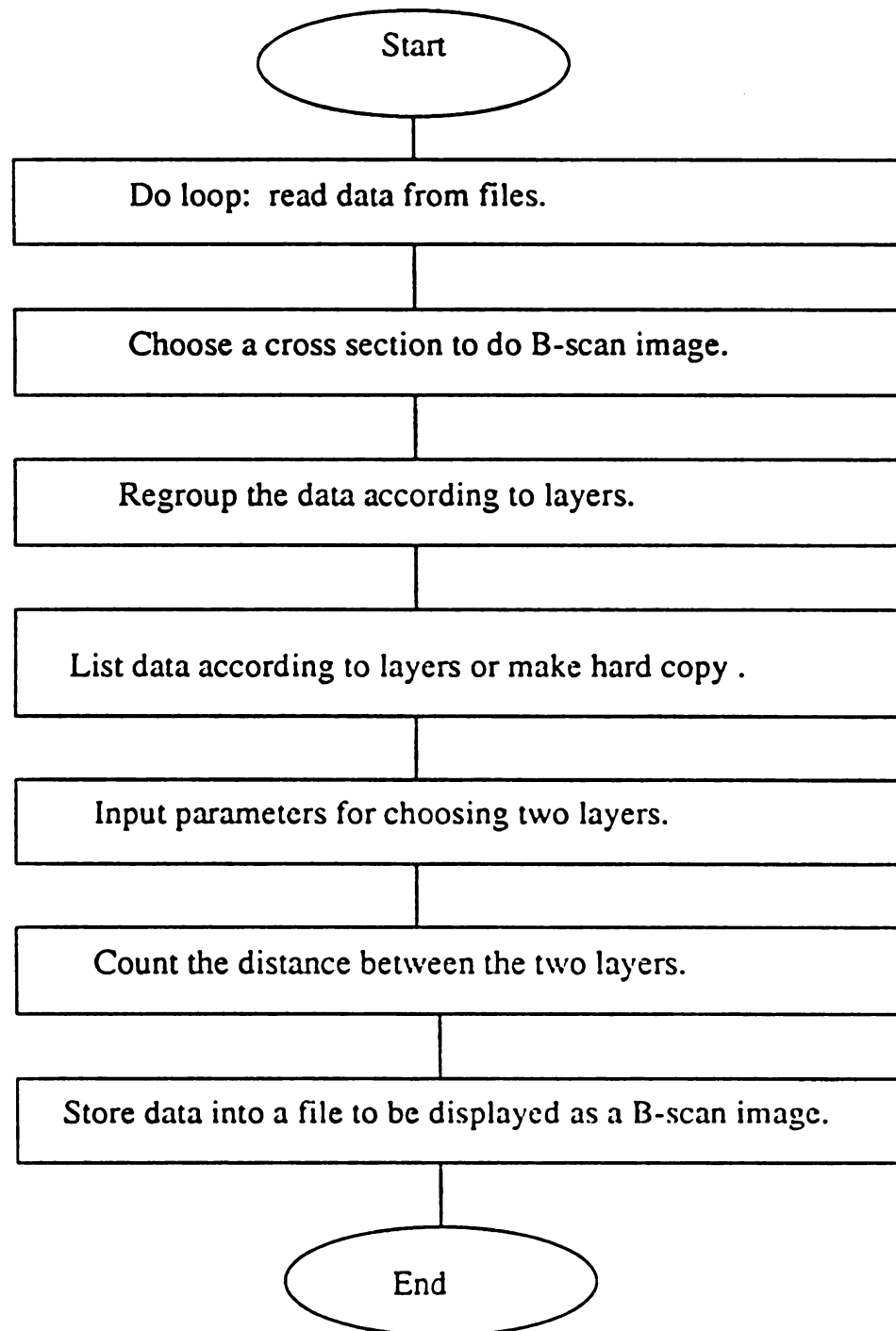
Figure 5.2.3   The program for processing B-scan data to find the velocity change due to temperature change.

CHAPTER 6

Experiment Design and Procedures

A set of experiments were done to verify the system capabilities of temperature measurement and to prepare for further biomedical applications. Experiments were conducted in which the temperatures were varied in a medium and the change in ultrasonic propagation velocity across that medium was recorded. These experiments will be described in the sequence of experiment configurations, data processing, results and discussion which follow.

6.1 Experiment 1: The ultrasound velocity change of oil due to temperature variation

This preliminary experiment is for verifying that the acoustic velocity changes in liquid due to a temperature variation. As mentioned before, the velocity of ultrasound in water increases with increasing temperature initially, reaches a maximum at a temperature around 80^0C, then decreases with further increase in temperature. For most liquids, however, the velocity of ultrasound in the liquid decreases with increase in temperature. Vegetable oil was used as an example to verify the ultrasound velocity variation with temperature in liquid.

The experimental set up is shown in Figure (6.1.1). A 2.25 MHz focused transducer is immersed in an oil box at a fixed position. A heater is used to increase the temperature of oil.

A mask, with a small hole which lets ultrasound through, is mounted on the transducer to provide a reference signal. The transducer launches a pulse and receives an echo signal. The system digitizes the echos and saves the data into a data file. Obviously, the time interval between the reference signal echo and the echo of the box bottom is determined by the ultrasound velocity. A typical echo return wave form is shown in Figure (6.1.2).

In the experiment, the oil was heated to temperatures of $10^0 C$, $15^0 C$, $20^0 C$ and etc. After an equilibrium is reached at each temperature, the system is triggered for 10 data files which are later processed.

Data processing is used to improve the accuracy of the signals. As shown in Figure (6.1.2), the signal is mixed with noise. One way to increase the signal-to-noise ratio is to use averaging of multiple returns. The zero mean stationary noise is averaged to zero so that the signal-to-noise ratio will increase by $\sqrt{N}$ if N signals are averaged.

When averaging multiple returns, the signal phase differences due to system uncertainty can cause data degradation. Thus signal phase alignment is necessary before signal averaging is undertaken. By calculating the

correlation between two signals, the phase difference is detected. The position of the peak value of the correlation function is the distance between these two signals. These two signal are then aligned according the distance and are averaged. At each temperature, 10 signals are averaged to reduce noise and achieve a clean signal as shown in Figure (6.1.3).

For the signal at a certain temperature, the wave propagation velocity can be calculated from the time interval between the target distance. The velocity change is related to the temperature change by the time interval change. To calculate the time interval from the reference mask and the bottom of the oil box to a precision of 1 sampling point (66 ns), autocorrelation was used for each averaged signal. Calculation results of autocorrelation are shown in Figure (6.1.4).
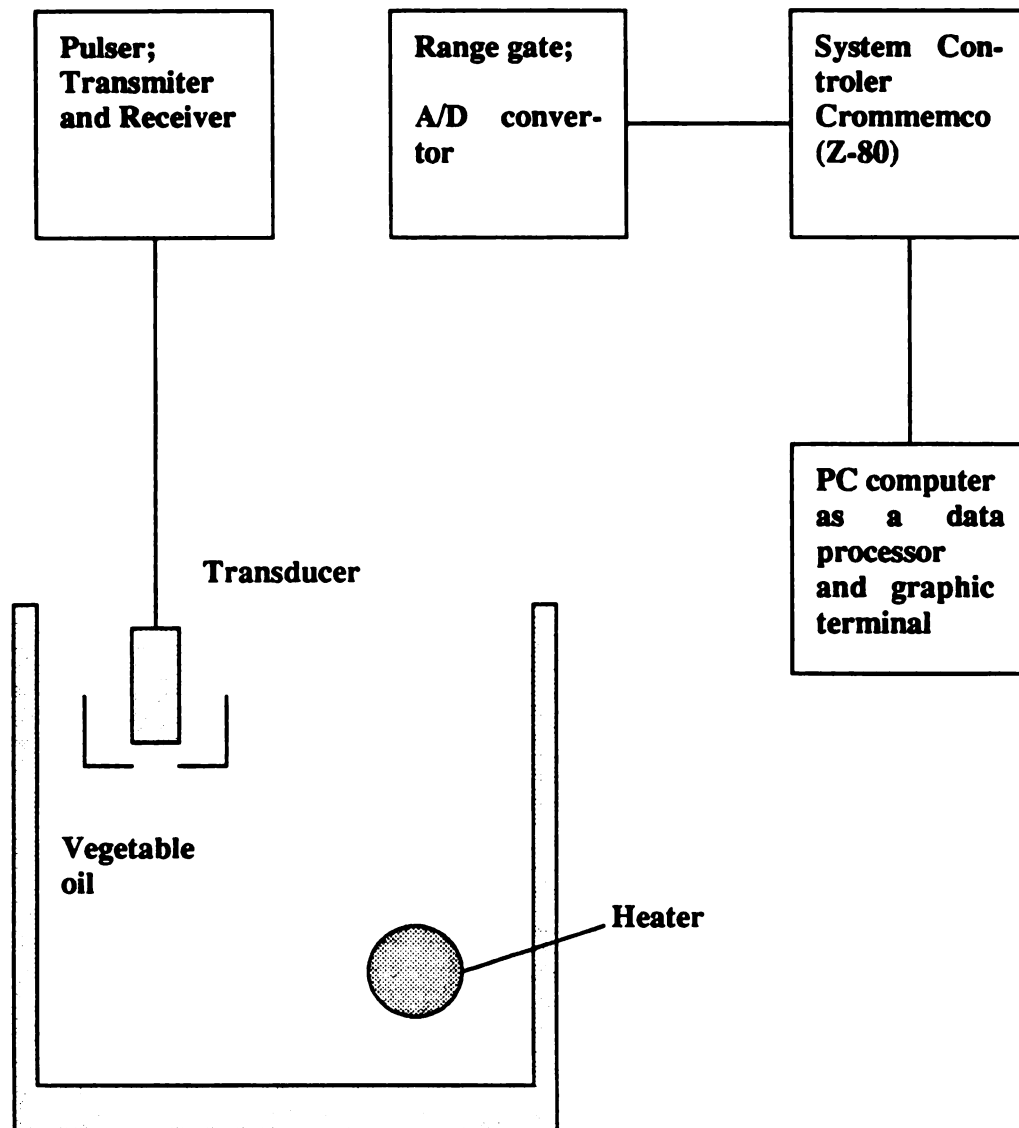
Figure 6.1.1 Experiment 1 set up. Test velocity dependency
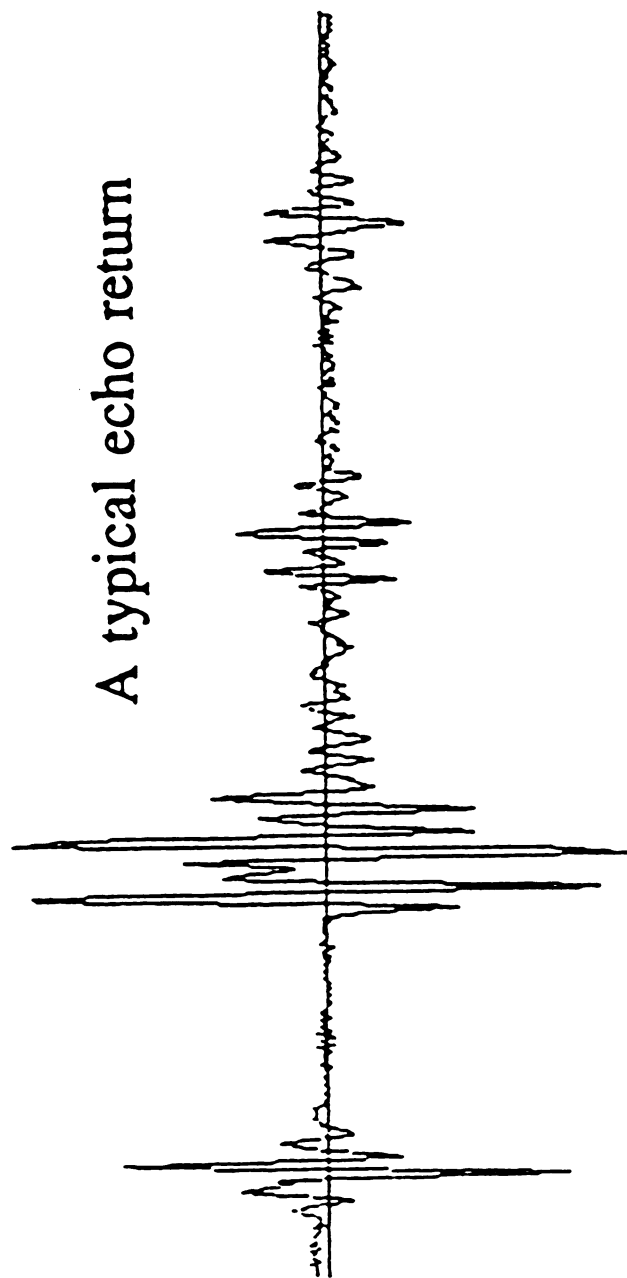on temperature for vegetable oil.

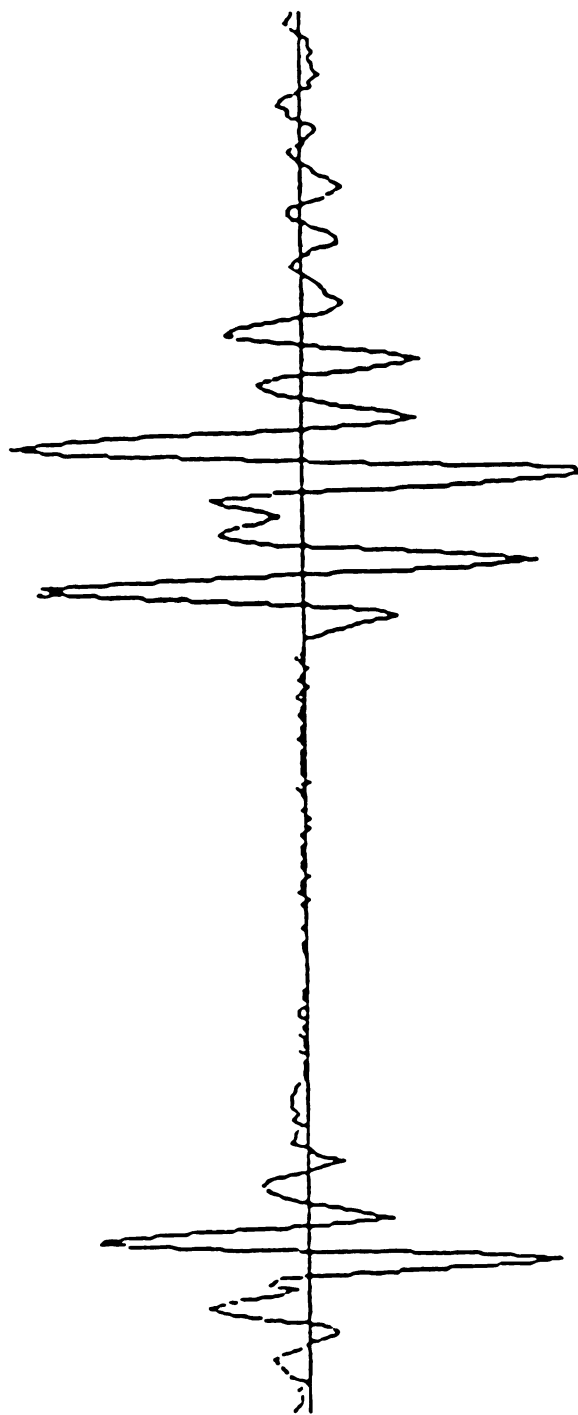Figure 6.1.2 The acoustic velosity change of oil due to temperature variation.
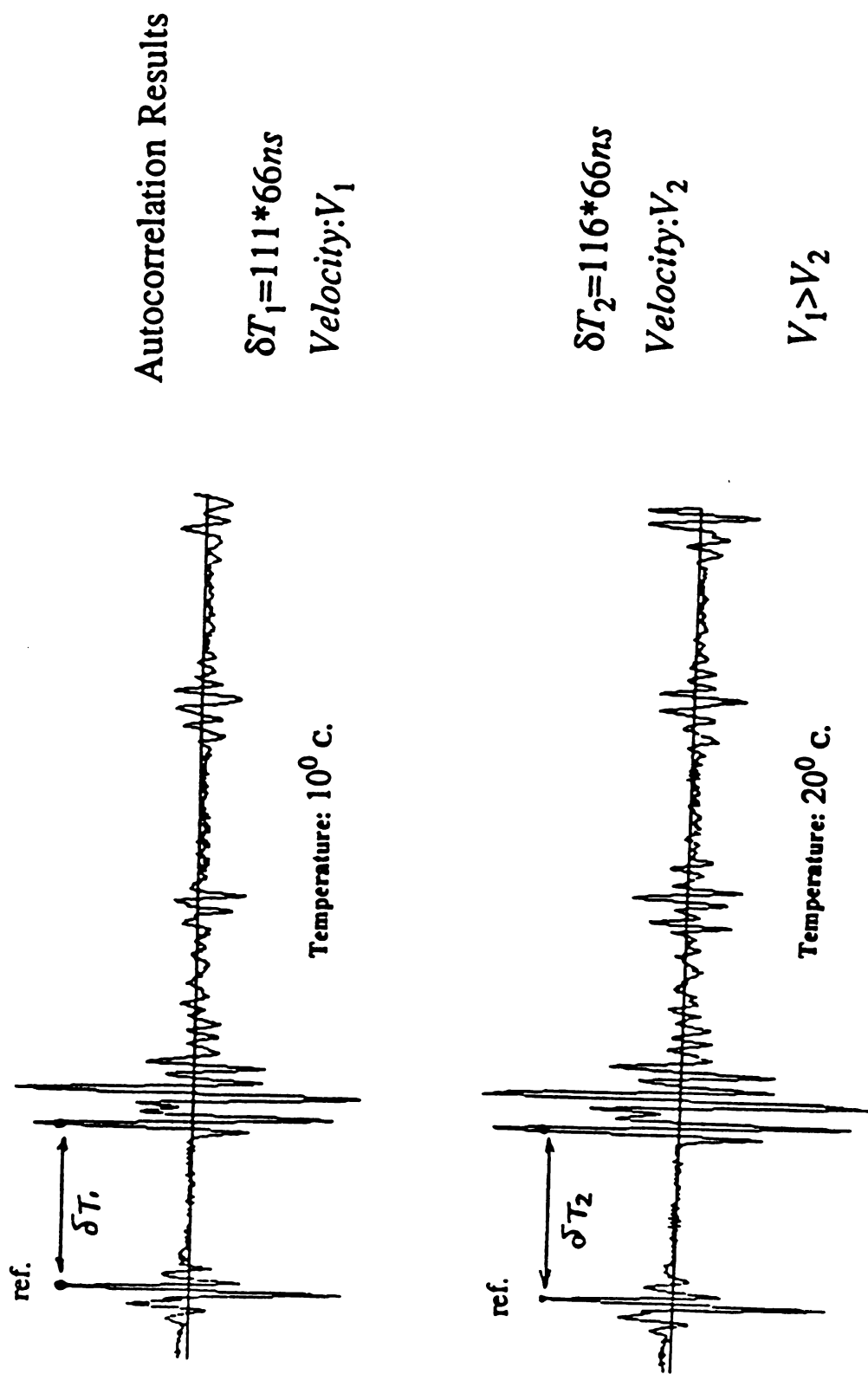
Figure 6.1.3   An echo return after averaging process.

71

Autocorrelation Results

$\delta T_1 = 111 \ast 66 ns$

Velocity:V_1

$\delta T_2 = 116 \ast 66 ns$

Velocity:V_2

$V_1 > V_2$

Temperature: 10^0 C.

Temperature: 20^0 C.

ref. δT_1

ref. δT_2

Figure 6.1.4   The autocorrelation results of the acoustic velocity change of oil due to temperature variation.

6.2 Experiment 2: Temperature profile in water

The purpose of this experiment with water was to verify that the system could indeed monitor a change in temperature and also could obtain a temperature profile in a medium by means of transducer scanning.

The experimental configuration is shown in Figure (5.1.1). A 2.25 MHz piezoelectric focused transducer was mounted to a scanner which was driven by stepmotors for 2-dimensional scanning in a degassed water tank. A plastic ice container for cooling and an electric heater were put at two opposite sides in the water tank. A plastic plate was located on the scan area to the system reflections from equal distances between the reflector and transducer. Thus the system should be able to detect any velocity change due to temperature change when an ultrasound wave propagates in the medium. The data from every position can then be used to obtain a temperature profile in the medium. Again, a physical reference (the mask previously discussed) is used to eliminate uncertainty in signal triggering.

During scanning, both the specimen and transducer are kept under water in the degassed water tank. The transducer is held above the specimen, usually at a height determined by the focal length of the transducer. The transducer is moved parallel to the surface of the plastic plate by two stepping motors which control movements in the X and Y directions.

Initially, the area of the specimen to be scanned is selected. The movement units are dependent on the step size of the motors , which is about 1mm/step. The spatial resolution is defined by specifying the intervals at which measurements will be recorded, the minimum spacing being 1mm. Once the initial parameters are set, the scanning process can begin.

During the scanning, the system controller triggers the transducer and receives all the echo signals from the specimen. Only the first echo is identified and stored into a file, accompanied by the X and Y location. This data file is then displayed as a three- dimensional image to represent the temperature profile in the medium. Figure (6.2.1) shows the constant temperature profile response.

To obtain a temperature gradient in water, an ice cooler was put on one side and an electric heater was turned on at the other side of the tank. A scan over this temperature profile give the results shown in Figure (6.2.2) when no reference signal is used. When the reference is used the results are as shown in Figure (6.2.3). As mentioned before, because of the triggering uncertainty, the travel time from the transducer to the reflector plate was affected by both system triggering uncertainty and velocity change. The triggering uncertainty is removed by the use of the reference signal, leaving only a variation due to temperature.

To compare the non-invasive measurement, with an invasive temperature measurement, as described in Chapter 5, the image in Figure (6.2.4) was obtained. The temperature profile for the invasive measurement looks smoother than that in Figure (6.2.3). One reason for this difference is that the probe of the fluoroptic thermometer not affected by the heat stream inside the water tank.
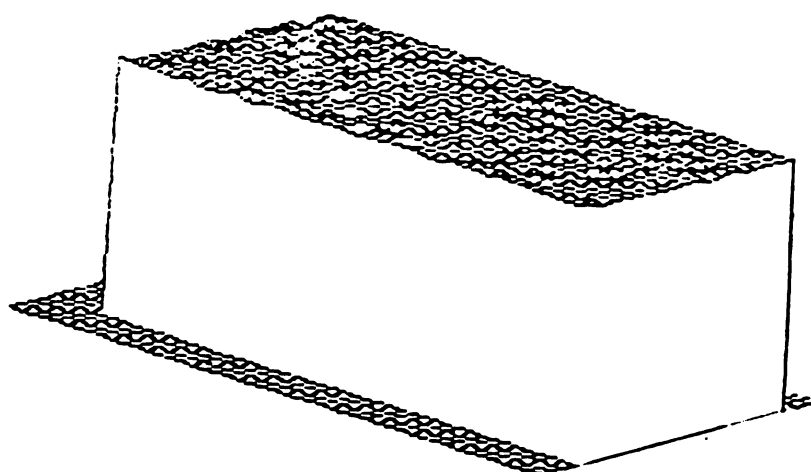
Figure 6.2.1   Three dimensional imaging for the constant temperature in water, using a reference signal.

Temperature profile of water without
the use of reference
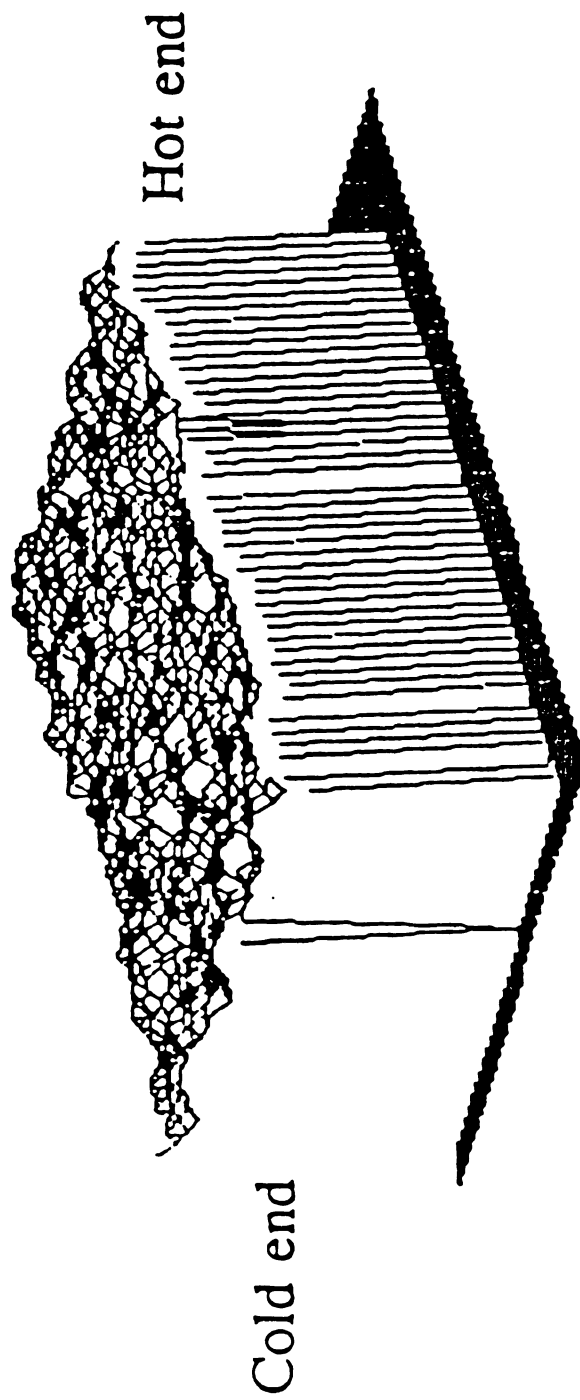
Hot end

Cold end

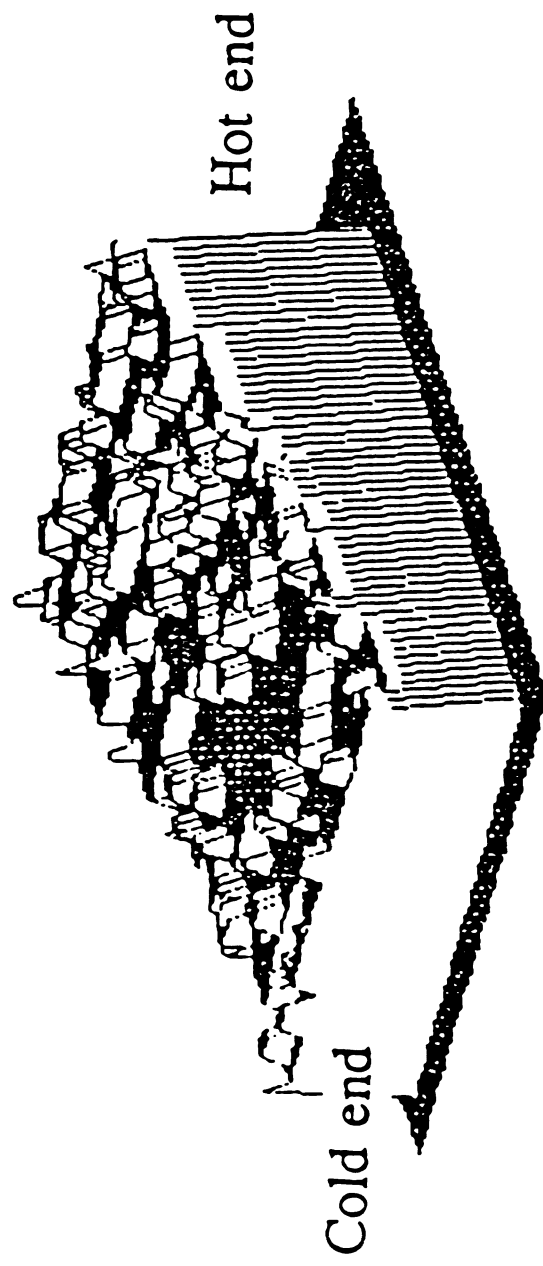Figure 6.2.2   Temperature profile of water without the use of reference signal.

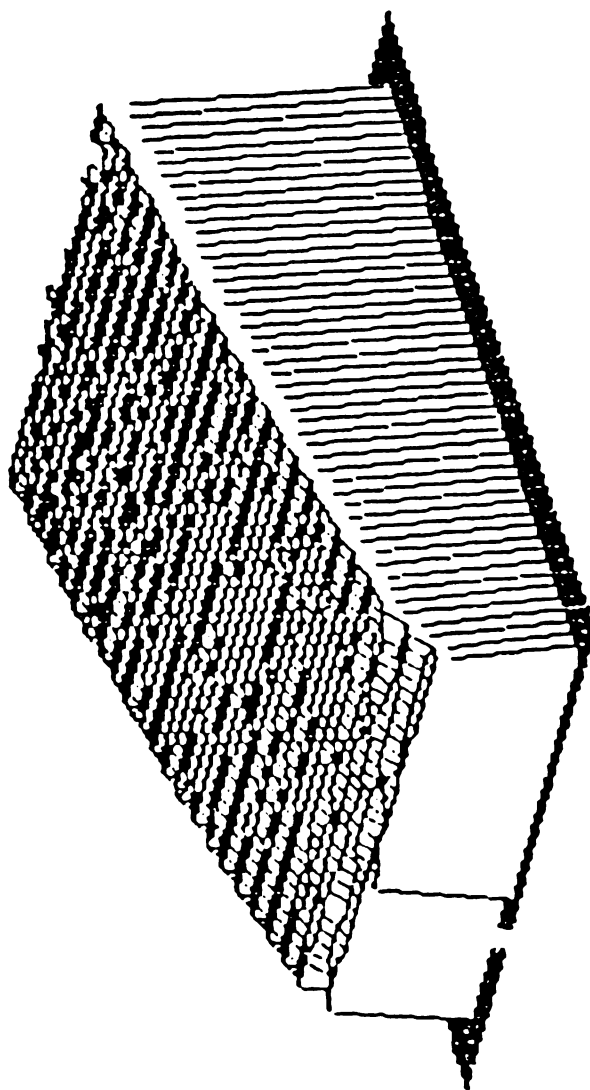Figure 6.2.3   Temperature profile in water with the use of reference signal.

Figure 6.2.4   Temperature profile in water by using fluoroptic thermometer.

6.3 Experiment 3: Temperature profile probing of a layered model

In this experiment, only the non-invasive measurement system is viable, the invasive measurement system, though it has higher resolution and more sensitivity, is impractical. The layered temperature gradient model was built using two plastic boxes. As shown in Figure (6.3.1), one box was glued to the top of the other. Two 25 ohm resistors connected to a variable voltage source were used as heaters. These two heater were placed at opposite sides to allow different temperature distributions. Scanning of the this model was initially done without a voltage applied. A program was developed to detect the boundary shift due to the temperature gradient in each layer. Since the data include 3-dimensional location information, the X and Y represent a certain cross section in a B-scan, while the Z is the boundary location. Figure (6.3.2.a) and (6.3.2.b) show the conventional B-scan displays for different temperature conditions. To present the experiment results as velocity profiles, the program processes the original data file and calculates the time interval between any two boundaries and stores it into a new data file along with the X and Y co-ordinates which then can be interpreted as the velocity at each position. The velocity change will be found by comparing the data files at different locations, and these difference can then be interpreted as relative temperature difference. The results for the first step are shown in Figure(6.3.3.a) and Fig. (6.3.4.a), in which the temperature profile

shows an almost constant temperature throughout the entire region.

In the second step, 50 volts was applied to each resistor for five minutes to create a temperature gradient inside the two boxes. As depicted in Figure (6.3.3.b) and Figure (6.3.4.b), the heater in the upper region was placed on the right-hand side, thus the temperature gradient results obtained were as expected. After heating, the temperature increases toward the right-hand side where the heater is located. By comparing two images, an exact temperature gradient or a relative temperature change can be identified. This relative temperature change monitoring alone would be a valuable tool for many applications. For the lower region, the heater was installed on the opposite side. Similarly, Figure (6.3.4.b) shows a temperature increment toward the left-hand side because of the position of the heater. The significance of Figure (6.3.4) is enhanced by the fact that it is a temperature profile of a sublayer, which is a more difficult region to monitor by conventional methods.
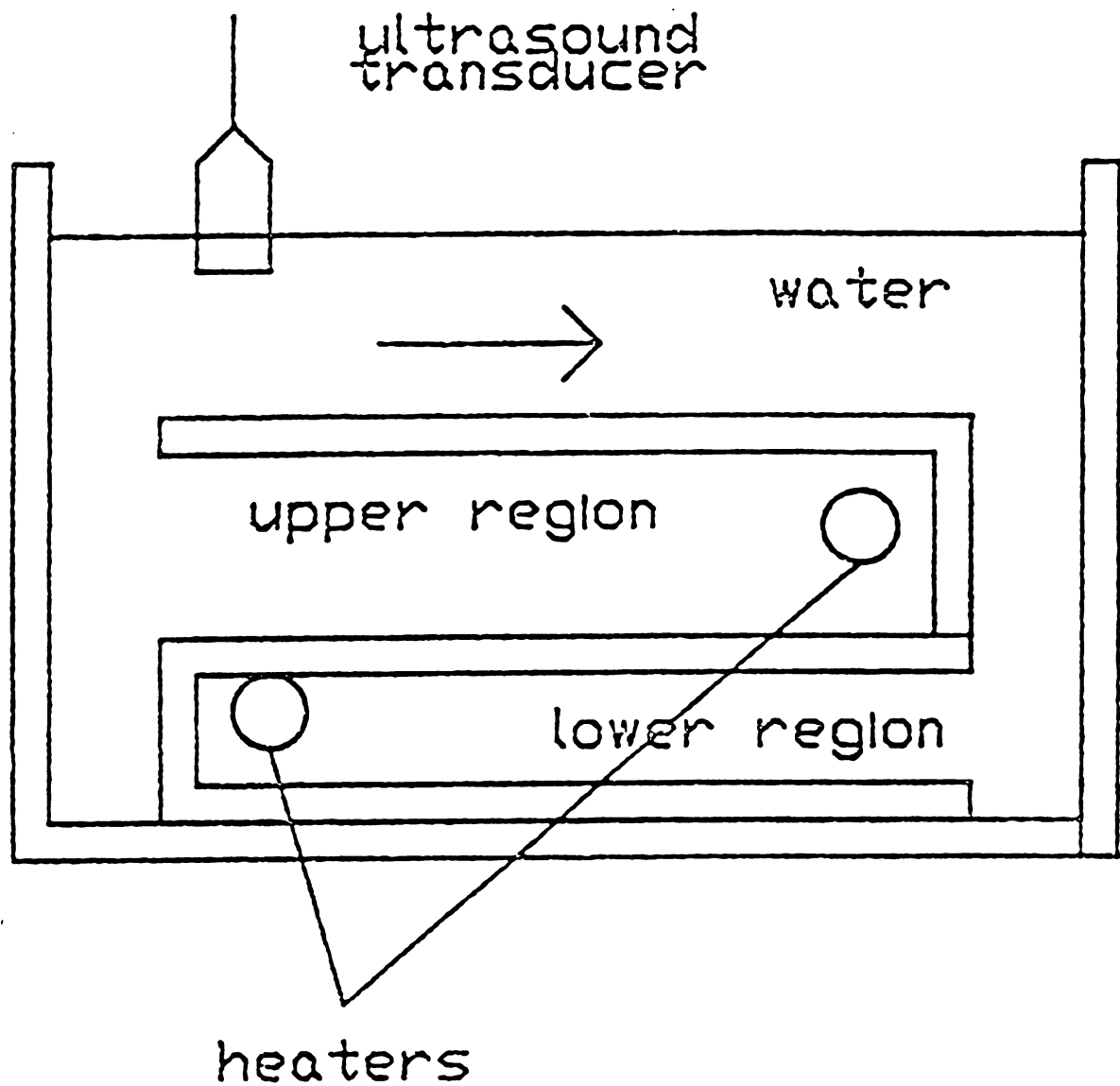
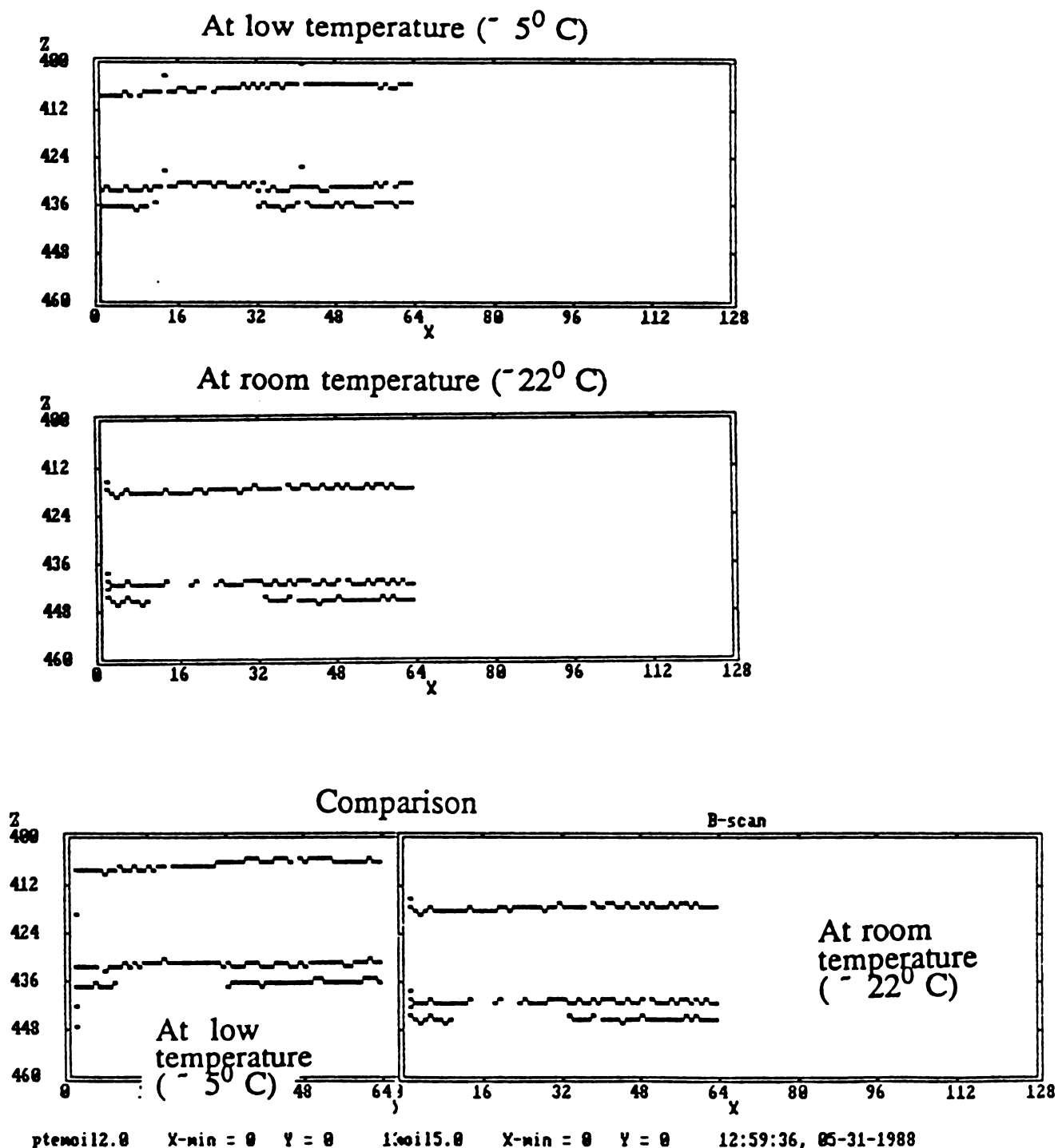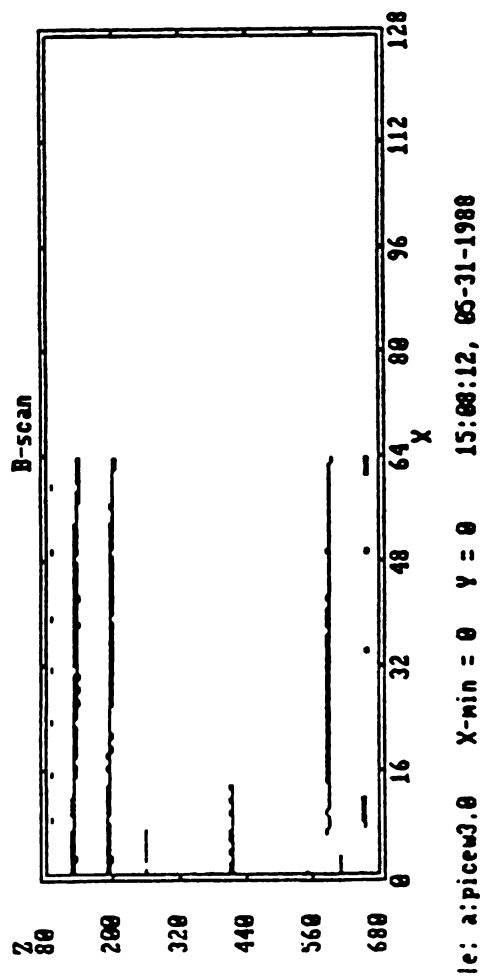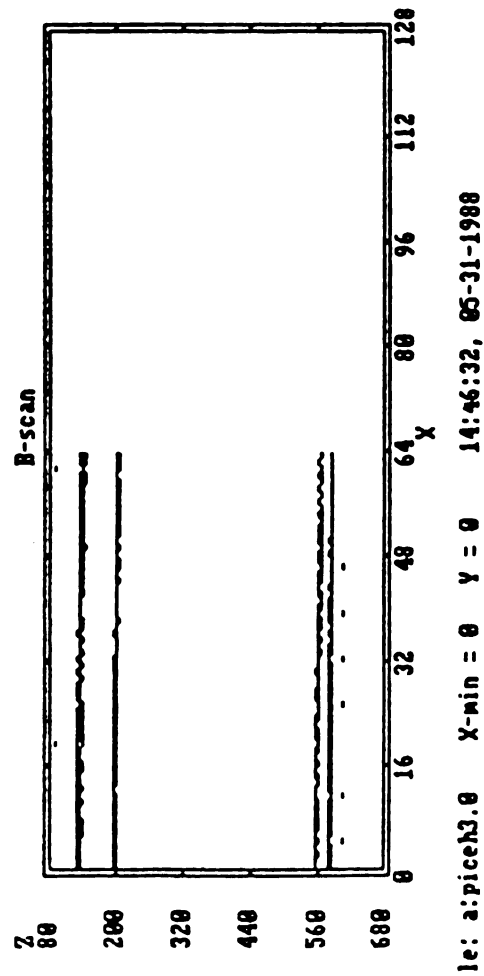Figure 6.3.1   A layered temperature gradient model.

Figure 6.3.2.a   B-scan image to show a boundary shift due to temperature change (X and Z coordinates are distance and wave traveling time respectively).

Scan a box with ice and water

water

Ice

B-scan

Z
80

200

320

440

560

680

0   16   32   48   64   80   96   112   128
X

le: a:picew3.0   X-min = 0   Y = 0   15:08:12, 05-31-1988
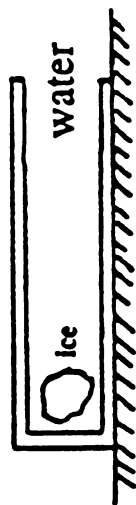
Scan a box with water at room temperature

water

B-scan

Z
80

200

320

440

560

680

0   16   32   48   64   80   96   112   128
X

le: a:piceh3.0   X-min = 0   Y = 0   14:46:32, 05-31-1988

Figure 6.3.2.b   B-scan image for temperature measurement.

(a) Temperature Profile of Upper Region without Heating

(b) Temperature Profile of Upper Region with Heating
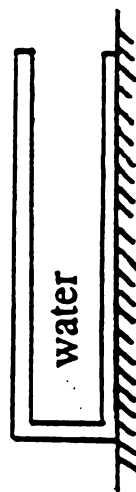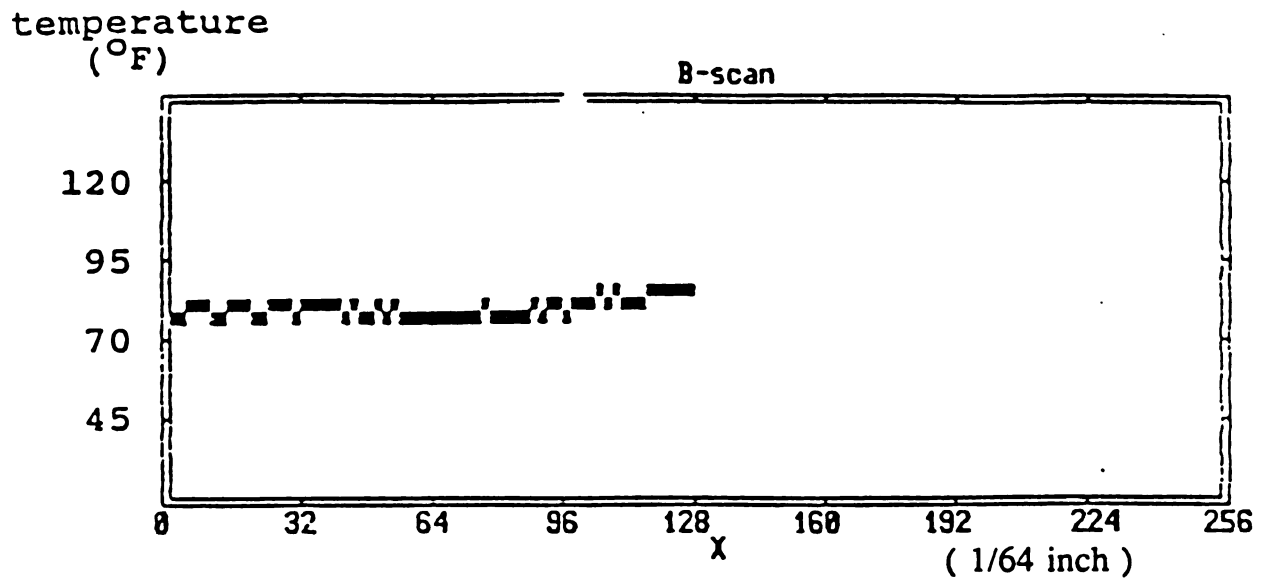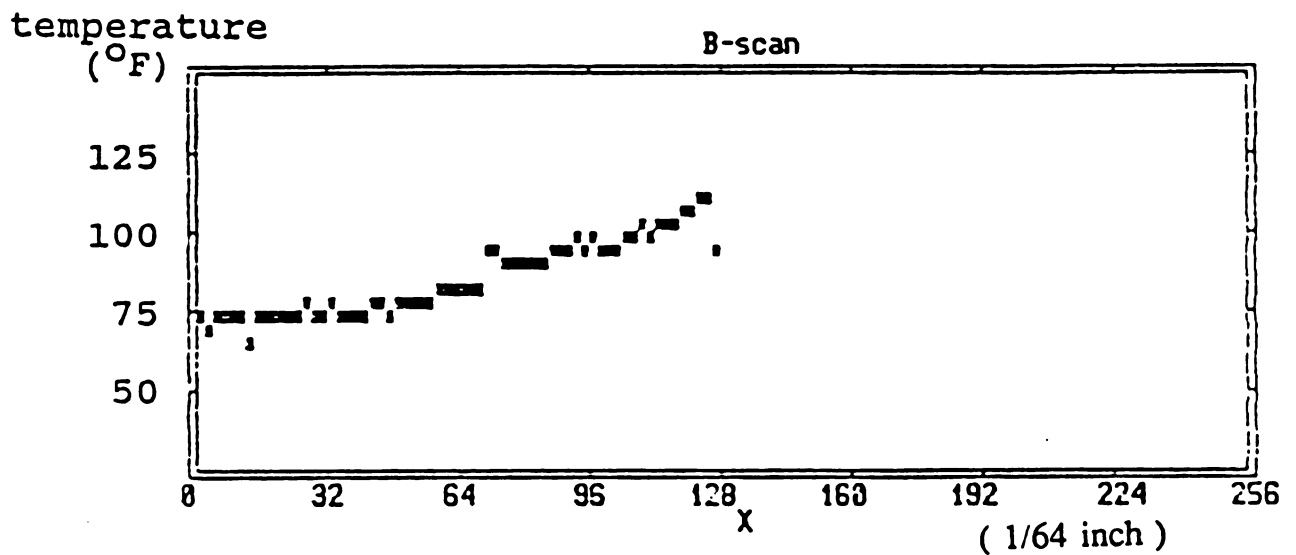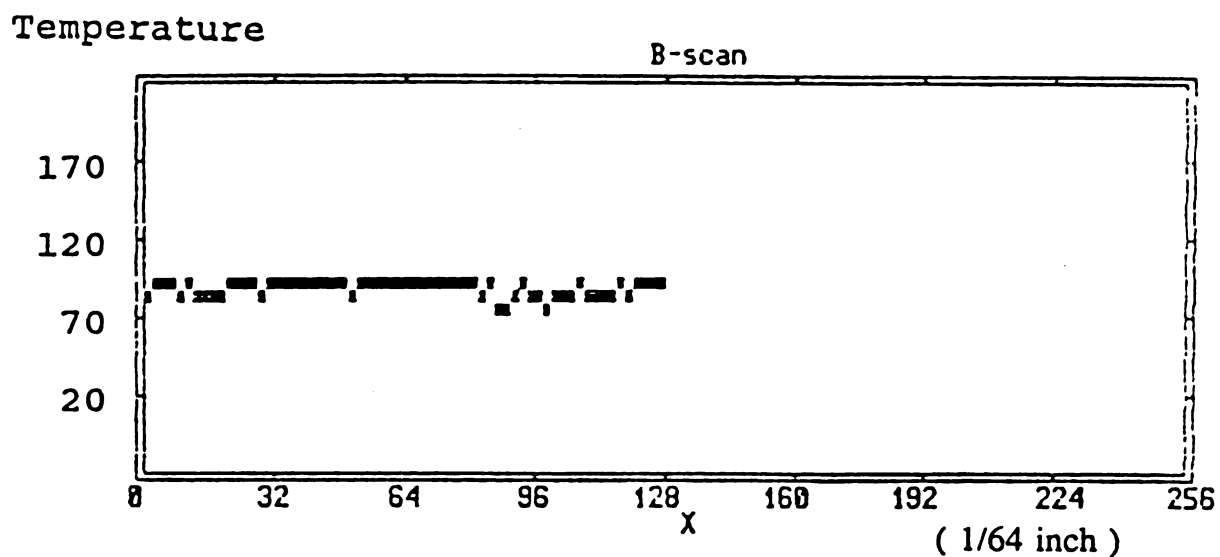
Figure 6.3.3   Temperature profiles of the upper region of the model.

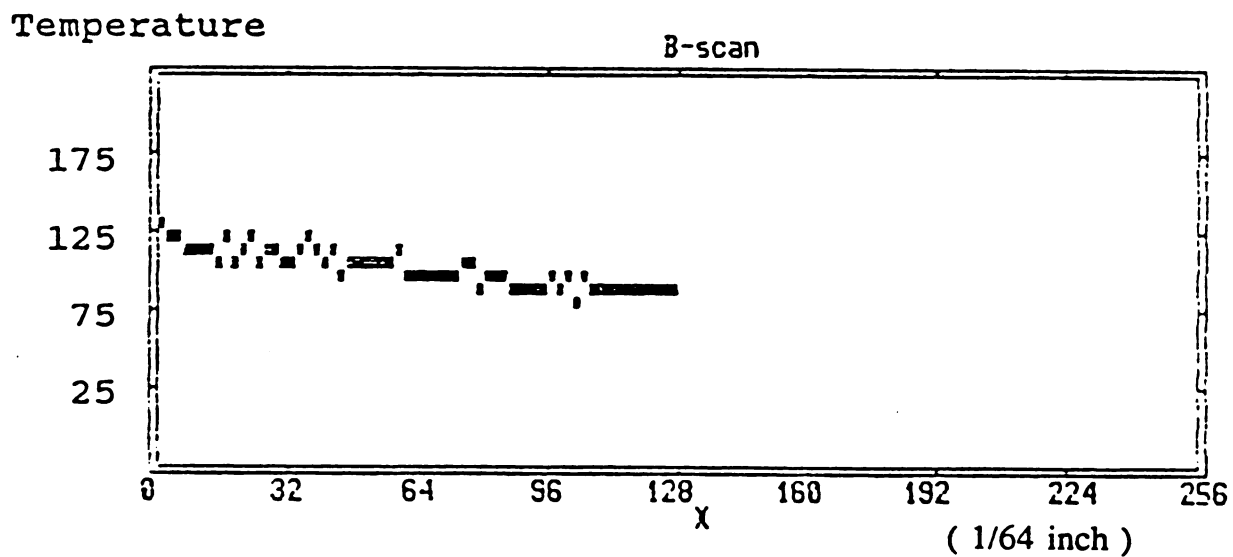(a) temperature profile of lower region without heating

Figure 6.3.4   Temperature profiles of the lower region of the model.

6.4 Experiment 4: Design Considerations and Procedural Aspects for Biomedical Tissue Studies

Ultrasonic non-invasive temperature measurement has become increasingly important as a monitoring method in hyperthermia treatment. Ultrasonic properties of many tissues have been reported by numerous authors which provide the experimental basis for measurement techniques. Many techniques developed in principle, however, still have not been implemented in medical applications despite the efforts of many investigators. The effect of temperature on ultrasonic velocity in biomedical tissues has been examined by Carstensen [13] and Bamber[14] and others. Preliminary findings indicate that ultrasound velocity in nonfatty tissues increases with temperature in the range from 5^0C to 50^0C for ultrasonic frequencies between 1 and 7 MHz. Figure (2.2.2) and (2.2.3) show that the expected temperature coefficients of velocity range is from 0.5 to 1.6 m/s^0C.

This experiment was designed to simultaneously simulates hyperthermia treatment and to monitor the change in propagation velocity as a function of temperature (which could be used for monitoring the temperature variation during hyperthermia treatment).

The experimental set up is shown in Figure (6.4.1). A specially designed degassed water tank was used for both hyterthermia treatment

simulation and for non-invasive measurements. A 2.25 MHz focused transducer which was 19 mm in diameter was fixed to the bottom of water tank to represent the treatment transducer. A constant amplitude signal generator, which generates continuous sine waves from 60 KHz to 100 MHz, and a power amplifier, were used to drive the transducer. The acoustic power output was calibrated experimentally by the radiation force method. A holder in the water tank is for mounting a specimen between the treatment transducer and the diagnostic transducer. Similar to previous experiments, a 2.25 MHz diagnostic transducer of 0.5 inch in diameter were above the specimen. A modified ultrasonic imaging system was utilized in this experiment. A state-of-art data acquisition board with a sampling frequency up to 40 MHz was installed in a PC micro-computer. This data acquisition board has less triggering uncertainty than the system used in previous experiments.

As depicted in Figure (6.4.1), the diagnostic transducer was aligned with the ultrasound treatment transducer on the bottom. A pork kidney was used as the specimen on a holder between the two transducers. A pulse was launched into the specimen by the diagnostic transducer before treatment insonation. The data acquisition board received, sampled the echos and stored them a file for later processing. The real time echo waveform is shown in Figure (6.4.2). The time interval between boundaries was used to

represent the velocity within the specimen, which can be mapped to temperature difference. The boundary defined here is the maximum peak in a local area, where the local area is defined as a period of 100 sampling points or so, depending on the echo waveform pattern. The starting point of a local area is the first peak whose amplitude is above the threshold.

After the first data file is stored, a ultrasonic insonation was done by the transducer on the bottom. A 2.25 MHz continuous sine wave was used for a duration of 15 minutes. The reading on the meter of the power amplifier was 20 watts which corresponded to 1 watt of acoustic power. A second data file was generated from data taken after the insonation. The velocity-temperature transformation algorithm described above was used for processing the two data files to find the velocity change inside the specimen caused by ultrasound induced heating. The results listed below are the boundary positions before insonation and the positions after. The positions represent the relative temperature change inside a pork kidney due to 15 minutes of ultrasonic insonation.

The data before insonation at water temperature of $21^o C$ resulted in the following boundaries:

boundary 1:   272 *samples*   (each sample equals 25 ns)

boundary 2:   517 *samples*

boundary 3:   1064 *samples*

The data after insonation at higher water temperature and higher kidney temperature gave:

boundary 1:   252 *samples*

boundary 2:   447 *samples*

boundary 3:   1031 *samples*

The time interval inside the specimen is 792 sampling points in the pre-insonation data and 779 sampling points after insonation. Assuming that the thickness of the specimen (about 2.5 cm) has not be changed, the velocity change through the travel region inside the specimen can be calculated as:

$$\Delta V = \frac{2.5 * 10^{-2}}{779 * 25 * 10^{-9}} - \frac{2.5 * 10^{-2}}{792 * 25 * 10^{-9}} = 21 m/sec.$$

It is readily simple to get relative temperature change from this velocity change if a calibrated relationship of velocity vs. temperature is available. Note that the surface boundary and bottom boundary are also shifted because of the temperature change along the water path. This result shows that the pulse-echo method used here is capable of detecting the temperature change inside a biomedical specimen provided that it does have clear boun-

daries.

In addition to the above experiment, several one-dimensional scans were done across the pork kidney. A round flat shape, electric heater was used below the kidney for heating. Again, the first scan was done before the heater was turned on to obtain a B-scan image. The second scan was done after the heater was turned on for 10 minutes. Figure (6.4.3) shows B-scan images of the kidney specimen for both cases. Since the heat conduction inside the specimen is slower than that of the water outside the specimen, all of the boundaries are shifted in the same direction which indicates that the temperature has risen in water, but the temperature change inside the specimen is not as obvious.
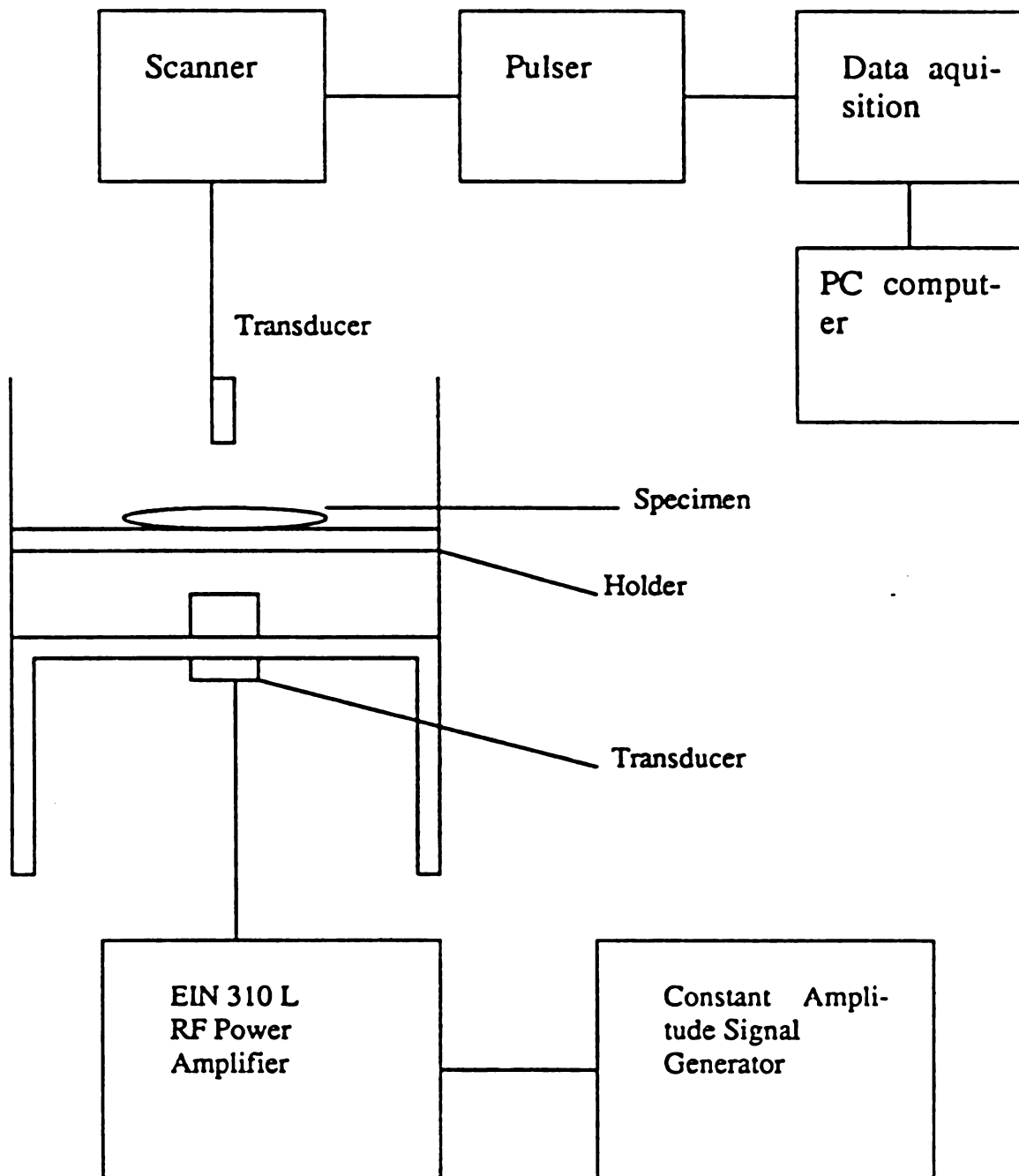
Figure 6.4.1 Experiment 4 set up for biomedical applications.
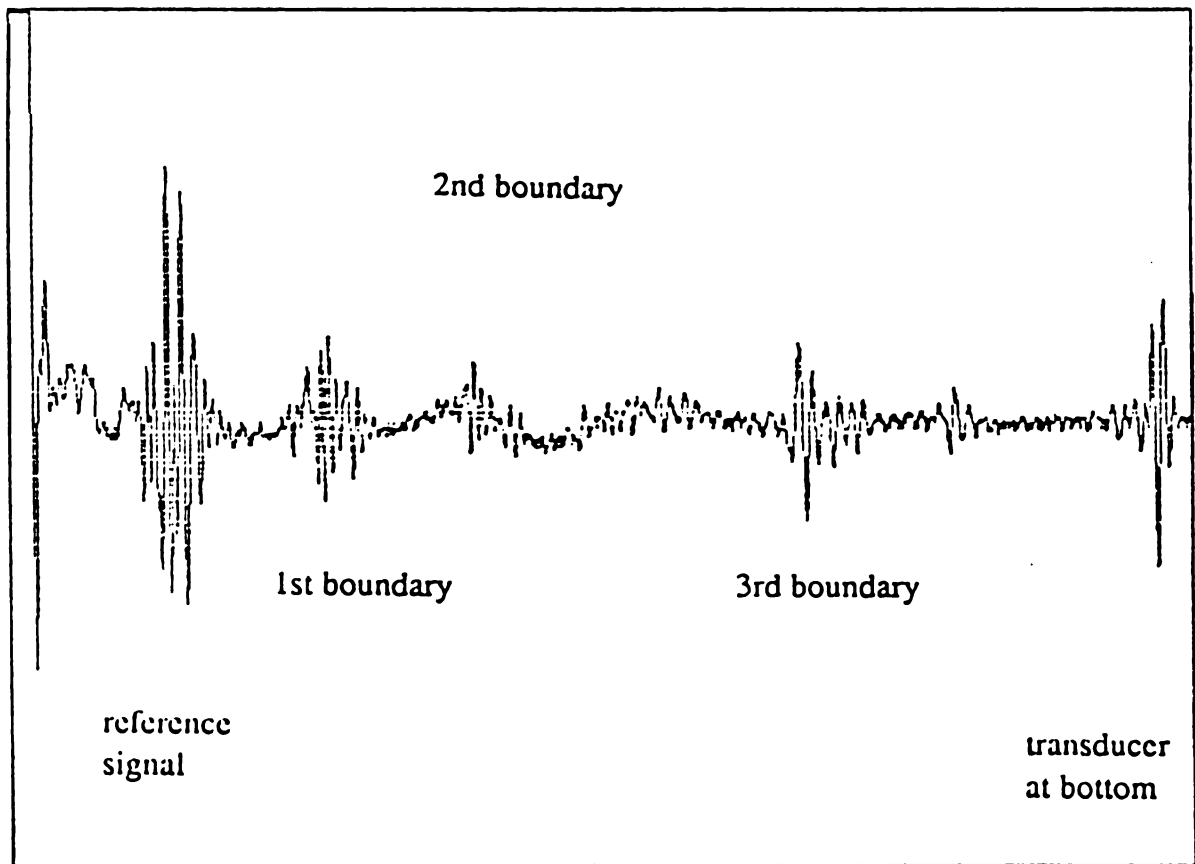
Figure 6.4.2 The echo waveform of a pork kidney specimen.
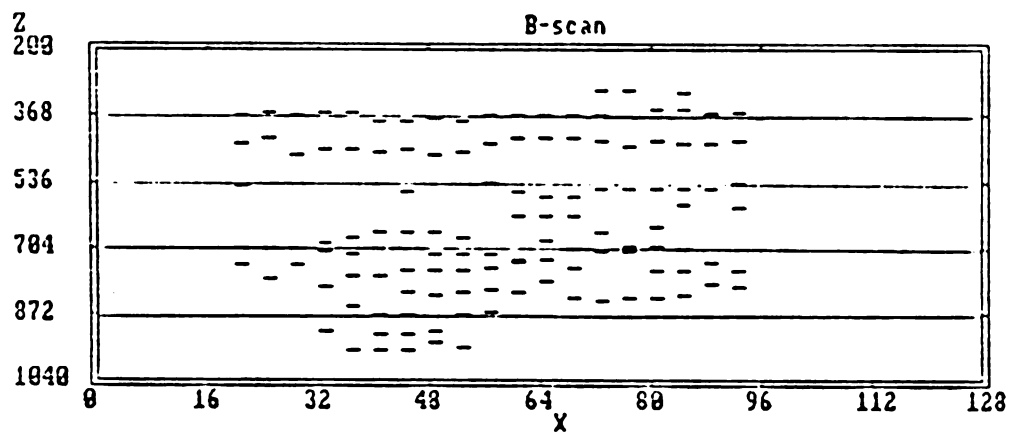
The image before heater turned on (temperature $22^o C$).
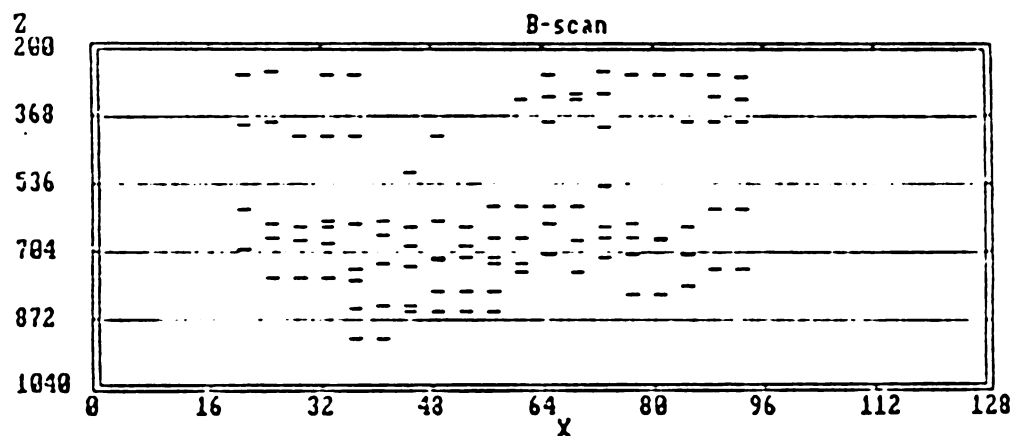
The image after heated for 15 minutes (temperature $29^o C$).

Figure 6.4.3   B-scan images of a pork kidney specimen to show the boundary shift due to temperature changes.

CHAPTER 7

Analysis of Experiment Results

7.1 Analysis and Discussion

The experiments with water demonstrated the ease with which a change in temperature can be detected by a change in the speed of ultrasound. Even though the experiments here were in a preliminary stage, without calibration for real application, it is necessary to investigate the accuracy and resolution possible and consider the requirements for future medical applications.

7.1.1 Accuracy and Time Resolution

The results described in Chapter 6 are actually an average temperature variation along the wave travel region. The accuracy is dependent upon the time resolution and the ultrasound wave travel region.

Based on previous results by B.J. Davis [10] and S.A. Johnson, the requirement for time resolution to determine temperature difference of various tissue sample widths is given in Figure (7.1.1)[15]. Extrapolation of the graph in the Figure to smaller ordinat values shows that with a time resolution of 1 ns for example, a $0.2^o C$ temperature change in a 4 mm diameter region can be detected in a tissue with a temperature coefficient of 3

m/sec$^o C$ (typical for water and biological tissues). With a time resolution

capability of 1 ns, an 8 mm diameter or larger region is necessary to produce

a 1 ns change in time-of-flight when the temperature changes by $0.1^o C$

within that region. The graph in Figure(7.1.1) shows the behavior of

$D = <V> \frac{\delta t}{(\delta V/V)}$, where D is the smallest diameter of a region where a

specific change in acoustic speed, $(\delta V/V)$, due to heating is just detectable

by a time resolution of δt. The average speed of sound, $<V>$, is taken to be

1500 meters per second. In table (7.1.1), the limitations of the system with

respect to detectable temperature changes are presented.

For those temperature change values listed in the table where the

change in propagation time is less than 25 ns (40 MHz sampling rate), the

current system cannot detect the associated temperature changes. Con-

versely, for changes in propagation time greater than 25 ns, the current sys-

tem can measure the associated temperature change. The heated area in the

kidney experiment 6.4 consisted of an area with 2 cm in diameter and had a

path length of about 3-4 cm. The resolution of temperature change in this

specimen would be about $1.0^o C$.

The final error in temperature determination in hyperthermia production

is a combination of calibration error and measurement error. A precision of

$0.2^o C$ to $0.5^o C$ might be required for useful systems. Clearly larger tem-

perature measurement errors can be tolerated below $42^o C$ while greater accuracy is required when approaching higher temperature where tissue damage can occur.

Acoustic velocity measurement techniques generally are able to measure changes in velocity much more accurately than absolute velocities. Some previous research concluded that the temperature coefficient of velocity is fairly constant for most tissues, but absolute propagation velocity is known to vary. From the point of view of medical application, information regarding initial body temperatures prior to treatment is important in order to determine the temperature rise from the therapy. Temperature measurements need to be done twice, before and after the therapy, to control the treatment procedure.

Table 7.1.1 Change in Ultrasonic Wave Propagation Times as a Function of Temperature Elevation and Path Length (All values in nanoseconds)

Path Length through the Region of Temperature Elevation

$\Delta T(^{\circ}C)$	1.0 cm	2.0 cm	3.0 cm	4.0 cm	5.0 cm	10.0 cm
0.1	0.67	1.33	2.00	2.67	3.33	6.66
0.2	1.33	2.67	4.00	5.33	6.66	13.33
0.5	3.33	6.66	10.00	13.30	16.70	33.30
1.0	6.66	13.30	20.00	26.60	33.30	66.60
2.0	13.30	26.60	39.90	53.20	66.50	133.10
5.0	33.10	66.30	99.50	132.70	165.80	331.70
10.0	66.00	132.00	198.00	264.00	330.00	660.00
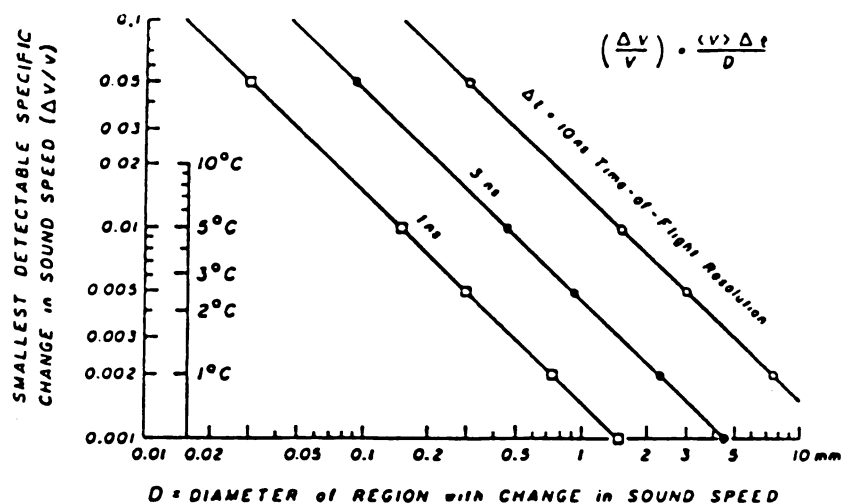
Graph of the smallest specific change in acoustic speed $\delta v/v$ which can be detected in a region of diameter D using a time of flight detector of resolution δt. The average speed of ultrasound is taken to be 1500 m/sec.

Figure 7.1.1 Effect of time-of-flight resolution on detectability of local ultrasound speed change in small region of given diameter.

7.1.2 Medical Applications

Medical application of the technique is not expected to be as straightforward as the experiments on biomedical tissues described above due to

1. temperature gradients occurring within the body,

2. unknown values of the temperature coefficient of velocity,

3. patient movement, and

4. complex boundary identification due to the degree of impedance mismatch and multiple echo returns.

For the pulse-echo measurement, in order to make relative velocity measurement it is necessary that:

(1) there exist a strong acoustic impedance mismatch at the treatment region from which a signal can be reflected,

(2) the capability of identifying boundary position despite complex waveforms from different tissues (due to the degree of impedance mismatch, wave dispersion and attenuation).

(3) an initial propagation velocity must be obtained prior to treatment, so the change in propagation time of the reflected signal can be related to a change in propagation velocity.

Impedance mismatch beyond the treatment region is assured by the presence of bone or air. In general, tumors which are accessible for

ultrasonic heating or visualization are also accessible for velocity measurement. Some less impedance mismatch problem did happen in experiment 6.4 when a pork liver specimen was used. There was no clear surface boundary appeared which was necessary for boundary shift detecting. In this case, as a compensative way, a reference signal might be used to obtain major boundary shifting information.

As has been stated, common values of the temperature coefficient of velocity range from 0.8 to 1.6 $m/(sec^{o}C)$ depending on tissue. In medical applications, the tumor temperature would be determined non-invasively by measuring the change in ultrasonic velocity in the tumor, calculating the corresponding temperature change from the known temperature coefficient of velocity and adding this value to the known initial temperature assumed to be at $37^{o}C$ for most circumstances. For the technique to be exclusively non-invasive and accurate, a better knowledge of the temperature coefficient of velocity is necessary.

Another problem which can limit the medical application of the above techniques is patient movement during hyperthermia treatment. The boundary echo shift is assumed to occur over a constant path length and is considered to be due to temperature changes alone. If the path length varies, however, the boundary shift can be misinterpreted as due to temperature change even if no change has occurred. Even movements as small as a few

tenths of a millimeter can lead to false temperature change calculations. A possible way to overcome this problem is to make velocity measurements synchronous with the respiratory or cardiac cycles. Another way to limit the false temperature reading is to ensure that the transducer and the internal body interface, serving as a reflector for the ultrasonic wave such as between bone and tissue are firmly fixed with respect to one another. This would allow some movement of intervening tissue but ensure that the ultrasonic propagation distance is constant as required. The greater the movement of the tumor during hyperthermia, the less likely these proposed correction methods will be effective. Treatment areas which are least effected by the movement problem are the limbs, lower abdomen, head and neck.

It is possible that in .the cases where knowledge of the temperature coefficient of velocity is good and patient movement is minimal, that the described non-invasive technique could be used as the exclusive means of non-invasive temperature measurement. In those cases where the temperature dependence is not well-known, the described technique could aid in the determination of tumor temperature using supplemental information obtained from invasive probes.

7.2 Conclusion and Future Study

Monitoring temperature variation inside material during processing is quite important in many applications. Since the non-accessibility in those cases where invasive measurement techniques using thermistors and/or thermal-couples are impractical, the non-invasive ultrasonic velocity method is a promising technique. This thesis outlined technique to measure ultrasonic velocity changes during hyperthermia (produced by scanning focused ultrasound). The pulse-echo mode is used to monitor the boundary shift due to velocity change, indicating the relative temperature change. This technique will not disturb the environment and will be benefit for patients in medical treatment. The pulse-echo method will provide greater potential than the transmitting method since it is more accessible in the human body.

The precision of the temperature measurement is directly related to the time resolution of the echo. Additional improvement can be achieved by using the data acquisition equipment with higher sampling rate and less triggering uncertainty. More experiments with biomedical tissues in-vitro under simulated hyperthermia, to get experimental models and data for future in-vivo experiments, are necessary.

To calibrate the measurement system, high precision fluoroptic thermometry should be used for comparison of temperature images. The tem-

perature coefficient of velocity in different tissues and the absolute tempera-

ture mapping algorithm must still be refined.

Bibliography

[1] Lele, P. F., *Physical Aspects and Clinical Studies with Ultrasonic Hyperthermia,* F.K. Storm Editor, G.K. Hall & Co. Boston, MA, 1983.

[2] Cetas, T. C. and Connor, W. G., *Thermometry Considerations in Localized Hyperthermia,* Medical Physics, 5, p79-91, 1978.

[3] Isaak E. Elpiner, *Physical, Chemical, and Biological Effects,* Consultants Bureau, N.Y., 1964.

[4] Wells P. N. T., *Physical Principles of Ultrasonic Diagnosis,* Academic Press. N. Y. p23, 1969.

[5] Lele, P.P., *Thresholds and Mechanisms of Ultrasonic Damage to Organized Animal, Tissues,* In Proceedings of a symposium of Biological Effects and Characterizations of Ultrasound Sources, 1977.

[6] Abramowitz, M. and Stegun, I.A., *Handbook of Mathematical Functions,* National Bureau of Standards, Applied Mathematics Series, p55, June, 1964.

[7] Wells, P.N.T., *Biomedical Ultrasonics,* Academic Press, N.Y. (1977).

[8] Papadakis, E.P., *Ultrasonic Velocity and Attenuation: Measurement Methods with Scientific and Industrial Applications,* Physical Acoustics Principles and Methods volume XII, W.P. Mason, Editor, Academic Press, New York (1977).

[9] Hull, D.R., et al, *Measurement of Ultrasonic Velocity Using Phase-Slope and Cross-Correlation Methods,* Materials Evaluation, v.43, p1455, October, 1985.

[10] Brian, J. D. and Padmakar P. Lele, *An Acoustic Phase Shift Technique for The Non-invasive Measurement of Temperature Changes in Tissues,* 1985 IEEE Ultrasonics Symposium, p921.

[11] Steven, A. J., et al, *Nonintrusive Acoustic Temperature Tomography for Measurement of Microwave and Ultrasound-induced Hyperthermia,* Journal of Bioengineering, Vol. 1, pp 555-570, 1977, Pergamon Press, Inc.

[12] Carstensen, E.L. and H.P. Schwan, *Acoustic Properties of Hemoglobin Solutions,* J. Acoust. Soc. Amer., vol.31, pp.305-311, 1959.

[13] Bamber, J.C. and C. R. Hill, *Ultrasonic Attenuation and Propagation Speed in Mammalian Tissues as a Function of Temperature,* Ultrasound Med. Biol., vol.5, pp. 149-157, 1979.

[14] Wang, Nai Hsien, *Remote Sensing by Acoustic Video Pulse Techniques,* A Thesis for Master of Science, Department of Electrical Engineering and System Science, Michigan State University, 1988.

[15] Johnson, S. A., and et al, *Non-intrusive Measurement of Microwave and Ultrasound-induced Hyperthermia by Acoustic Temperature Tomography,* IEEE Ultrasonics Symposium Proceedings, pp. 977, 1977.